LEVEL II

IMS

INSTITUTE OF MATERIALS SCIENCE

THE UNIVERSITY OF CONNECTICUT
Storrs · Connecticut

UC-MET-KAT-4-1981

(7)

FINAL REPORT

INTERACTION OF MICROSEGREGATION AND COARSENING DURING DENDRITIC NICKEL-BASE ALLOY MONOCRYSTAL GROWTH

GRANT AFOSR 77-3344

April 1, 1977-August 31, 1981

October 31, 1981

Submitted to

Air Force Office of Scientific Research
Department of the Air Force
Bolling Air Force Base, D.C. 20332

T. Z. KATTAMIS

INTERACTION OF MICROSEGREGATION AND COARSENING DURING DENDRITIC NICKEL-BASE ALLOY MONOCRYSTAL GROWTH

ABSTRACT

Dendritic monocrystals of various Ni-Al-Ta and Ni-Al-Cr alloys, some of which were microalloyed with C,B,Zr or Hf were processed at various growth rates up to 200 cm/h ,or cooling rates up to 4.44 K/s under a thermal gradient in the mushy zone of 80 K/cm and in some cases 180 K/cm. The solidification microstructure was substantially refined with increasing growth rate and dendrite arm spacings as fine as 1 to 2 μm were observed in laser or electron beam surface glazed monocrystals, corresponding to local cooling rates in excess of 10^5 K/s. Microsegregation of Al,Ta and Cr was found to depend on growth conditions. With increasing cooling rate, within the range of those encountered in monocrystal processing the volume fraction of nonequilibrium interdendritic γ-γ' eutectic or secondary γ' increases. At the high growth rates achieved in surface glazing this volume fraction is greatly reduced. Very high growth rates are required for complete elimination of interdendritic γ' through solute trapping,and formation of a completely homogeneous surface layer. Such high rates could be reached during glazing. With the present chilling techniques available growth of homogeneous monocrystals at such high rates, which would enhance productivity,is not possible. Homogeneous monocrystals could ,of course, be processed at extremely low growth rates yielding plane front solidification. This solution would be detrimental to productivity.

Extremely short solution and homogenization treatments are sufficient for homogenizing the fine microstructure of rapidly

solidified monocrystals and the ultrafine microstructure of surface glazed material.

Dendritic coarsening kinetic studies led to the following conclusions: (1) At a given cooling rate an increase in Ta concentration refines the microstructure more than does an equal percental increase in Cr concentration and much more than does an equal percental increase in Al concentration; (2) Further dendritic refinement is achieved by microalloying with C,B,Hf or Zr and; (3) Suppression of convection in the liquid has a refining effect on the dendritic microstructure.

FINAL REPORT

SUMMARY

I. INTRODUCTION

This four year program, initiated April 1, 1977 and completed August 31,1981 has been focused on the solidification microstructure and microsegregation in ternary nickel-base alloy dendritic monocrystals. The main objectives of this investigation were:

1) To establish the dependence of solidification microstructure on process variables:Thermal gradient in the mushy zone,G, growth rate, R, hence cooling rate G·R, alloy composition and microalloying. Since dendritic coarsening is the mechanism that controls the fineness of solidification microstructure the investigation was primarly involved with determining the effect of process variables, especially composition and microalloying on coarsening kinetics.

2) To establish the dependence of microsegregation, expressed by the extent of dendritic coring and by the volume fraction of interdendritic nonequilibrium γ-γ'eutectic or secondary phase γ' on process variables.

3) To evaluate the dependence of solution and homogenization kinetics on initial microstructure, hence on process variables during monocrystal growth.

4) To extend these findings to ultrafine microstructures processed by laser or electron-beam glazing dendritic monocrystals or polycrystalline material.

This investigation was extended to two commercial superalloys, IN-100 and B-1900. The ultimate objectives of this investigation were the control and optimization of microstructure and its fineness, the minimization of microsegregation and the reduction in duration of post-growth solution and homogenization treatments.

A summary of results of the four year program is given below.

II. Ni-Al-Ta ALLOY SYSTEM

A. Coarsening Kinetics During Dendritic Monocrystal Solidification

A detailed analysis of the experimental procedure used, of the coarsening model adopted and of the dependence of coarsening kinetics on composition were reported in a publication (1).

The application of coarsening kinetic equations to the Ni-Al-Ta system requires the knowledge of the values of certain parameters, such as liquidus slopes and equilibrium partition ratios. The nickel-rich corner of the phase diagram of this system is only partially established and information on such parameters is not available. It, therefore, became necessary to derive[1] this information first: Twelve alloys were prepared, nine of which are represented by black circles in Fig. 1 and the three remaining are represented by black squares, A, B, and C. The liquidus temperatures of these twelve alloys were determined by differential thermal analysis. This determination led to plotting the lines 1685 (L), 1693 (L) and 1696 (L), which are basal projections of intersections of the liquidus surface with isothermal planes at 1665, 1693 and 1696 K.

The information derived and included in Fig. 1 may prove very useful for various studies on Ta-containing commercial nickel-base superalloys.

The effect of coarsening on the dendritic geometry of Ni-13.4at%Al-1.8at%Ta ingots grown at 0.25 m/h and coarsened for 0, 10 and 90s prior to quenching the remaining liquid is illustrated in Figs. 2(a), (b) and (c). Fig. 2(d) illustrates a typical photomicrograph of an isothermal cross-section taken within the mushy zone and used for evaluating the specific dendritic interface, S_v (dentrite-

liquid interface area per unit volume of solid).

Results of this investigation may be summarized as follows:

(1) The dimensionless specific interface, S_v/S_{v_o} decreases with isothermal coarsening time, Fig. 3. This decrease depends strongly on composition. Both analytical curves and experimental points clearly show that:

(a) At constant tantalum concentration (curves B and A) an increase in aluminum concentration slows down coarsening, yielding finer dendritic microstructures,

(b) At constant aluminum concentration (curves B and C), an increase in tantalum concentration drastically slows down coarsening, and

(c) At equal atomic percental increase in concentration, the effect of tantalum in refining the dendrite monocrystal microstructure is more significant than that of aluminum.

(2) Isothermal coarsening rate increases with temperature between the solidus and the liquidus, Fig. 4.

The previous conclusions are valid also for coarsening during solidification, Fig. 5, provided the initial 5 to 10s are excluded.

B. Microsegregation During and After Solidification of Dendritic Monocrystals-Solutionizing Kinetics.

Details of the investigation of microsegregation during and after solidification of dendritic monocrystals of Ni-Al-Ta as a function of growth conditions are included in a previous publication[2]. Dendritic monocrystals continuously grown prior to quenching, as well as others coarsened prior to quenching, Fig. 6, were used in this investigation.

The refinement of the dendritic microstructure with increasing

average thermal gradient within the mushy zone, G, and increasing growth rate, R, is illustrated in Fig. 7. The following dependence of primary dendrite arm spacing, d_1, on G and R was established:

$$d_1 = 4.37G^{-1.362}R^{-0.233}$$

The effect of composition on primary dendrite arm spacing was not very clear.

The segregation ratios of both aluminum and tantalum, $S = C_M/C_m$, where C_M and C_m are maximum and minimum solute concentrations, respectively, were found to slightly increase with increasing local cooling rate, $\varepsilon = G \cdot R$, Figs. 8 and 9, because of the shorter times then available for back diffusion of solute in the solid. The volume fraction of interdendritic nonequilibrium γ' phase, which is also an expression of the extent of microsegregation increases with local cooling rate too, Fig. 10.

Dendritic monocrystal solidification lends itself very conveniently to solution kinetic studies of the interdendritic nonequilibrium γ' phase during crystal pulling. For this purpose various cross-sections corresponding to known temperatures, hence times during pulling, were used, Fig. 11. The variation of fraction residual nonequilibrium interdentritic γ', g/g_o, where g_o is the volume fraction at the completion of solidification, versus time during monocrystal pulling is illustrated in Fig. 12. It is clear that solution kinetics are faster for the rapidly pulled crystal, presumably because primary dendrite arm spacing is then finer and so is the diffusion distance over which aluminum has to diffuse during dissolution of γ'.

In order to study the isothermal solution kinetics of interdendritic γ' dendritic monocrystals were pulled and the pulling was arrested for various lengths of time prior to quenching the remaining

liquid. Fig. 13 illustrates the variation of g/g_o versus isothermal holding time, temperature and microstructure. Data from Figs. 12 and 13 were replotted in Fig. 14 versus ϕ/L^2, where $\phi = D\theta$ for isothermal dissolution, θ is holding time, D is diffusivity of aluminum at the corresponding temperature and L is half the corresponding primary dendrite arm spacing. For dissolution during continuous pulling, $\phi = \int_o^{\theta_1} D d\theta$. A unique curve can be plotted across these points. Hence, solution kinetics depend only on the dimensionless parameter $D\theta/L^2$. This emphasizes the practical importance of very fine initial microstructures which require much shorter times for complete dissolution of the nonequilibrium interdendritic γ' phase. By reducing the dendrite arm spacing by half, the dissolution time is reduced by 75 pct.

C. Homogenization of Dendritic Monocrystals

Chemical homogeneity of an alloy has a beneficial effect on its mechanical properties. A fine cast microstructure and a uniform distribution of alloying elements within the dendritic γ-phase are highly desirable. Details of the study of homogenization kinetics of dendrite monocrystals of Ni-Al-Ta can be found in a publication on the subject[3].

A detailed diffusion model was introduced whose analysis resulted in the prediction of the dependence of the "index of residual segregation", δ_i, on homogenization time. This index, δ_i, for a solute, i, has been defined as:

$$\delta_i = \frac{C_M^{\theta} - C_m^{\theta}}{C_M^{o} - C_m^{o}}$$

where, C_M and C_m are the maximum and minimum solute concentrations measured after a time, θ , of homogenization, and C_M^o and C_m^o are the corresponding initial concentrations. At the beginning of the homogenization treatment $\delta_i = 1$. If complete homogenization has been achieved, $\delta_i = 0$. Fig. 15 illustrates the variation of δ_{Al} and δ_{Ta} with θ/ℓ^2, where ℓ is half the primary dendrite arm spacing. The importance of a fine dendrite spacing is emphasized by this figure. For an ingot solidified at 1.38×10^{-5} m/s under a gradient of 16×10^3K/m, $\ell = 8.9 \times 10^{-5}$m. After a homogenization treatment at 1588 K for 1h, a length of time which is industrially acceptable, the indices of residual segregation for aluminum and tantalum are $\delta_{Al}=0.3$ and $\delta_{Ta}=0.9$. Tantalum continues to be substantially segregated. Assume now that the ingot was solidified under the same gradient of 16×10^3K/m at 1.38×10^{-3} m/s , a high speed which can be achieved in a furnace equipped with a liquid tin-chill. In this case, $\ell = 5.5 \times 10^{-5}$ m and for a similar homogenization time $\delta_{Al}=0.04$ and $\delta_{Ta}=0.69$. The distribution of aluminum is now completely uniform. Tantalum is still segregated but significantly less than in the previous case.

During crystal pulling an appreciable homogenization of aluminum, the fast diffusing species takes place. That of tantalum is by far less significant. An examination of the geometry of the γ' precipitate shows very clearly that particle size depends on location within the dendritic structure, hence on local aluminum and tantalum concentrations. Figs. 16a and b show that the γ' particle size is finer in the center of dendrites, where concentrations of aluminum and tantalum are lower and coarser

in the interdendritic spaces where these concentrations are higher. The same observation can be made at a higher magnification in Figs. 17a and b, which also show the existence of a second generation of fine γ' precipitate between the coarser particles. While the coarser generation precipitated during continuous pulling of the monocrystal, the finer generation formed during quenching. It appears that in regions which are richer in solute the solvus temperature is higher and γ' precipitation occurs earlier than in regions which are poorer in solute. Thus, coarsening of the precipitate operates for a longer time in interdendritic regions and this explains why particle size is coarser in these regions (average particle size = 1.4×10^{-6} m) compared with that in the center of the dendrite (average particle size = 0.87×10^{-6} m). No significant variation of the vol%γ' was found across the dendritic structure.

As illustrated in Fig. 17c the distributions of γ' particles across the γ matrix and of the γ' particle size become more uniform after homogenization. This is understandable because after the homogenization treatment the distribution of solute, hence the solvus temperature and coarsening time are more uniform. The mechanical behavior of precipitation-hardened alloys is known to depend on precipitate particle geometry. It can be speculated that the beneficial effect of homogenization on properties of nickel-base superalloys is, at least partly, due to the above-mentioned effect of the treatment on γ' particle size and distribution.

III. Ni-Al-Cr ALLOY SYSTEM

A similar investigation was conducted on the Ni-Al-Cr system. Dendritic monocrystals of Ni-14.0at%Al-4.2at%Cr,Ni-18.0at%Al-4.1at%Cr, Ni-14.0at%Al-8.2at%Cr, Ni-19.2at%Al-11.9at%Cr and Ni-14.8at%Al-8.2at%Cr were solidified under a thermal gradient of $8x10^3$ K/m and at growth rates of 0.05, 0.10, 0.25 and 2.00m/h, prior to quenching the solid-liquid interface. The monocrystals were sectioned at different temperature levels at the time of quench and the distribution profiles of aluminum and chromium across each section were established by electron microprobe analysis. Transverse section made below the ternary eutectic temperature were used for measuring the volume fraction of tne remaining undissolved nonequilibrium γ' phase and establishing its solution kinetics during crystal pulling. For studying the isothermal solution kinetics of interdendritic γ' pulling of the monocrystals was arrested at a given moment for different lengths of time prior to quenching the remaining liquid. The remaining volume fraction of interdendritic γ' was measured in cross-sections corresponding to the same temperature in the various specimens and plotted versus holding time. Cross-sections taken within the mushy zone were used for studying the isothermal coarsening kinetics of the solid at various temperatures between the liquidus and the eutectic temperature[1]. This was done by measuring the solid-liquid interface area per unit volume of solid, S_v, at various locations corresponding to these temperatures in all specimens and plotting these data versus isothermal coarsening time.

Results from this investigation will be published elsewhere[4] and may be summarized as follows:

1) In plotting dendrite arm spacings versus growth rate or local cooling rate, cellular dendritic spacings should be reported on the secondary dendrite arm spacing curve. This was established as follows: The growth conditions corresponding to the morphological transition between cellular and columnar dendrites for Ni-18.0at%Al-4.1at%Cr alloy are shown in Fig.18. Among the five monocrystals processed, monocrystal A was grown under $G=8x10^3$ K/m and R=0.25m/h and monocrystal B under $G=20x10^3$ K/m and at R=0.10 m/h. The corresponding local cooling rate, $\dot{\varepsilon}$, for both monocrystals was therefore the same and equal to 0.55 K/s. Photomicrographs of longitudinal and transverse sections of these monocrystals are shown in Fig. 19. Monocrystal A is columnar dendritic and B is cellular dendritic. The cellular dendritic spacing in monocrystal B is equal to the secondary dendrite arm spacing in monocrystal A, not to the primary. This would indicate that coarsening, which is known to control secondary dendrite arm spacing, controls also cellular dendrite spacing in cellular dendrites. Fig. 20 illustrates the dependence of primary and secondary dendrite arm spacings, and of cellular dendritic spacing on growth velocity for two gradients: $8x10^3$ and $20x10^3$ K/m. For each gradient the cellular dendritic spacings fall on the extension of the secondary dendrite arm spacing curve. The critical growth rates R_1 and R_2 at which the transition between cellular dendritic and columnar dendritic structures occur for G_1 and G_2, respectively are indicated in the same figure. These values were deduced from

Fig. 18. The data points of Fig. 18 were reported in Fig. 21 versus local cooling rate $\varepsilon=G\cdot R$. Again secondary dendrite arm spacings and cellular dendritic spacings fall on one and the same curve, and primary dendrite arm spacings on another.

2) At constant chromium concentration (curves A and B), Fig. 22, an increase in aluminum concentration slows down coarsening; at constant aluminum concentration (curves B and C) an increase in chromium concentration slows down coarsening more significantly and; at equal atomic percental increase in concentration the effect of chromium is more significant than that of aluminum. A comparison with the coarsening behavior of the Ni-Al-Ta alloy system clearly shows that an increase in tantalum concentration slows down coarsening, yielding finer microstructures more substantially than does an equal atomic percental increase in chromium concentration.

3) There is a slight increase in segregation ratios of aluminum and chromium with increasing local cooling rate.

4) There is an appreciable increase of the volume fraction nonequilibrium interdendritic γ' phase, g_o, with increasing local cooling rate, Fig. 23.

5) The isothermal solution kinetics of the nonequilibrium interdendritic γ' in Ni-Al-Cr alloys are similar to those in Ni-Al-Ta alloys.

6) Aluminum homogenizes faster than chromium within the dendritic γ phase as predicted analytically and confirmed experimentally, Fig. 24.

Dendritic monocrystals of Ni-9wt%Al-4wt%Cr in which C,B,Zr or Hf were added to levels of 0.3% and 1.0% were directionally

solidified. Microsegregation of these elements and their effects on microsegregation of aluminum and chromium, as well as on the coarsening behavior of the dendritic γ phase were investigated. A paper is now in preparation[5]. The main results are:

1) Microalloying with these elements yields dendrites which exhibit tertiary arms and a higher initial specific interface, S_{V_O}, Fig. 25. Dendrite arm spacings are finer by about 5-10% than in absence of these elements. Their major role seems to be the decrease in solid-liquid interface energy which brings about slower coarsening kinetics and a finer dendritic microstructure.

2) B,Zr and Hf segregate at interdendritic spaces and grain boundaries. Their presence does not affect the microsegregation of aluminum and chromium in any appreciable extent.

IV. IN-100 ALLOY SYSTEM

An investigation of the dependence of solidification microstructure of dendritic monocrystals on growth parameters was conducted on an industrial alloy, IN-100 focusing, in particular, on the geometry and nature of the MC carbide. Results of this investigation were published elsewhere[6].

Carbides of the MC-type, which form during solidification of nickel-base superalloys, contribute to strengthening of grain boundaries at elevated temperatures. This strengthening role seems to depend significantly on carbide geometry. Also, fatigue life in alloys, such as MAR-M200 was found to be greatly affected by the size of preexisting cracks in MC-type carbide. The occurrence of such cracks prior to testing again depends on carbide

shape and size. Matrix slip and crack initiation often occur at precracked MC carbides and, to only a lesser extent, at micropores.

The microstructure of a unidirectionally solidified ingot in the vicinity of the quenched interface is illustrated in Fig. 26. This figure exhibits on the left side a longitudinal section of the ingot, and on the right, a series of transverse sections taken at various locations: A-A', B-B', C-C' and D-D', as indicated on the longitudinal section. A group of aligned, coarse faceted carbides appear in the quenched liquid ahead of the dendrite tips, section A-A', Fig. 26a. These carbides, which in subsequent fatigue testing were found to be associated with crack formation, were MC type "unmelted" carbides. At a further distance from the dendrite tips a "blocky" MC carbide appears, section B-B', Fig. 26b. This faceted carbide under appropriate G/R conditions grows as a "chinese script"-type carbide, Fig. 27. Further away from the dendritic tips appears the γ-γ' eutectic, section C-C', Fig. 26c over a temperature interval of a few degrees. At the end of this interval a ternary γ-γ'-MC eutectic sometimes appears. Results of the study on carbide shape, size and composition may be summarized as follows:

(1) The volume percent of faceted carbide decreases with increasing growth and decreasing thermal gradient, hence with decreasing G/R ratio, Fig. 28a.

(2) The average faceted carbide size decreases with increasing growth rate, R, and increasing thermal gradient, G, hence with increasing cooling rate, $\varepsilon = G \cdot R$, Figs. 28b and c.

(3) The specific perimeter of faceted carbides increases with growth rate and thermal gradient, hence with cooling rate, Fig. 28d.

(4) The chinese script-type carbide spacing becomes finer with increasing growth or cooling rate.

(5) The corresponding molecular formulas of these three types of carbide are, $(Ti_{0.70}Mo_{0.16}V_{0.06}Cr_{0.02})C$, with minor amounts of cobalt and zirconium for the faceted carbide, $(Ti_{1.76}Mo_{0.03}V_{0.05}Cr_{0.02})C$, with minor amounts of cobalt and zirconium, for the unmelted faceted carbide and $(Ti_{0.76}Mo_{0.15}V_{0.06}Cr_{0.03})C$, with minor amounts of cobalt and zirconium, for the chinese script-type carbide. It can be seen that the unmelted faceted carbide is richer in titanium, and poorer in molybdenum and vanadium than the faceted carbide which grew from the melt during solidification at a temperature below the liquidus of the dendritic γ-phase. These unmelted carbides often contain alumina cores, on which the carbide nucleated heterogeneously during an earlier stage in the processing of the master alloy.

Similar composition measurements were conducted on carbides in various specimens grown at different rates and under different gradients. No significant variation of composition was found with growth conditions.

IV. B-1900 ALLOY SYSTEM

A parallel investigation was conducted on B-1900 alloy. Results were similar to those obtained with IN-100 and a publication is now in preparation[7].

V. RAPIDLY SOLIDIFIED TERNARY NICKEL-BASE ALLOYS

A. Solidification Microstructure of High Energy Beam Glazed Ni-Al-Ta and Ni-Al-Cr Dendritic Monocrystals and Polycrystalline Plates.

There are expectations and already some indications that substantial strengthening can be achieved through rapid quenching. This strengthening could be attributed to : 1) A refined dendritic microstructure and a more uniform distribution of solute, hence a more uniform intragranular strength; 2) a smaller volume fraction of interdendritic secondary phase which contributes to a reduction in ductility; 3) an extension of equilibrium solid solubility leading to an increase in solid solution strengthening; 4) a refinement of the cast grain which is oberved only in some cases and; 5) a possible effect of rapid solidification on phase changes in the solid.

The results discussed earlier in this report were extrapolated toward higher cooling rates by rapidly remelting and resolidifying dendritic monocrystals and polycrystalline plates of Ni-13.1at%Al-5.1at%Ta and Ni-21.0at%Al-8.0at%Cr with a continuous wave CO_2 highly focused laser beam[8] delivering a power of about 4.7 kW. Beads of 1.5,1.42,1.2, 1.08 and 0.69×10^{-4}m maximum depths and of very fine microstructure were produced at travel speeds of 0.125, 0.254, 0.380 and 0.508 m/s. A parallel investigation[9] was conducted on electron-beam glazed specimens of Ni-9.0wt%Al-4.0wt%Cr containing nominally 1.0wt%C ,B or H_f. These specimens were scanned transversely by an electron beam 3×10^{-4} m in diameter, operated at a power level of 300W and at velocities of about 0.054, 0.08, 0.217 and 0.402 m/s.

The following are the main results of this investigation:

1) The cellular-dendritic microstructure of the beads is very fine, Figs. 29 to 31, with dendrite arm spacings of about 1μm,Fig.32.

2) Microalloying with C,B or Hf further refines the cellular-dendritic microstructure ,Fig. 32, by slowing dendritic coarsening.

3) Microsegregation,expressed by the volume fraction nonequilibrium interdendritic γ' phase,g_o, is greatly reduced at high local cooling rates (10^5 to 10^6 K/s) achieved in high energy beam deposited beads. Thus,whereas g_o=0.06 at a cooling rate of 4 K/s, it is reduced by 50 pct, to 0.03 at a cooling rate of $7x10^5$ K/s [8]. At the bottom of shallow beads where cooling rate exceeds 10^6 K/s, a featureless zone appears, Fig.29. In this zone no microstructure has been resolved and there is no segregation of γ'. There are indications that this homogeneous zone consists of supersaturated γ-phase.

4) The dissolution times of nonequilibrium γ' in these very fine microstructures at elevated temperatures are very short of the order of a few seconds.

5) The beads exhibit banding, which consists of a periodic variation of microstructural fineness, Fig.31 and is associated with periodic macrosegregation [8,9].

CONCLUDING DISCUSSION

Rapid solidification of dendritic monocrystals of Ni-base alloys is particularly attractive because it yields finer cast microstructures and leads to higher productivity. Unfortunately, for the range of growth rates (or cooling rates) achieved, microsegregation increases with increasing rate. Microsegregation is deleterious to the mechanical and high temperature oxidation behavior of these alloys. It can be eliminated by a post-solidification solution and homogenization treatment whose duration must be limited,because of energy consumption and in order to limit solid state coarsening of various

dispersed nonmetallic phases, such as carbides, carbonitrides and others. In rapidly solidified monocrystals the dendritic microstructure is very fine and the treatment time is substantially reduced. Further refining of these microstructures can be achieved by adjusting alloy composition and by microalloying with elements, such as C,B ,Hf or Zr, which have also the additional beneficial effect of grain boundary strengthening.

On the basis of ongoing work it was concluded that at growth rates in excess of about 600 cm/h microsegregation in dendritic monocrystals would decrease with increasing growth rate and finally vanish for a growth rate of about 100 m/h. A completely homogeneous microstructure would then result. This critical growth rate could be reduced to about 10 m/h by raising the thermal gradient to about 800 K/m. Such values of growth rate and gradients cannot be achieved with the present types of chills used, including liquid Sn or Ga chilling. The next best solution would be to glaze the monocrystals using a high energy beam and scanning their surface. The ultrafine surface microstructure is less segregated than the bulk monocrystal and can be homogenized by very short treatments lasting only seconds at temperature. There are reasons to believe that such an epitaxial coating would improve the high temperature fatigue behavior and oxidation resistance of the monocrystals.

REFERENCES

1. P.W.Peterson,T.Z.Kattamis and A.F.Giamei,Met. Trans.A,Vol.11A, 1980,p.1059.

2. R.Kadalbal,J.J.Montoya-Cruz and T.Z.Kattamis, Met.Trans.A, Vol.11A,1980,p.1547.

3. G.D.Merz,T.Z.Kattamis and A.F.Giamei,J. Mater. Sci.,Vol.14, 1979,p.663.

4. J.J.Montoya-Cruz,R.Kadalbal,T.Z.Kattamis and A.F.Giamei, submitted for publication,Met.Trans.A.

5. R.Kadalbal and T.Z.Kattamis, in preparation.

6. R.Fernandez,J.C.Lecomte and T.Z.Kattamis,Met.Trans.A,Vol.9A, 1978,p.1381.

7. W.Schnake,T.Z.Kattamis and A.F.Giamei,to be submitted for publication,Met.Trans.A.

8. R.Kadalbal,J.J.Montoya-Cruz and T.Z.Kattamis,Proceedings of the Materials Research Society Symposium,Cambridge,Massachusetts, November 26-30,1979,Academic Press,Inc.,1980,p.740.

9. R.Kadalbal,J.J.Montoya-Cruz and T.Z.Kattamis, Proceedings of the 2nd International Conference on Rapid Solidification Processing, Reston,VA,March 1980,"Rapid Solidification Processing, Principles and Technology II",Claitor's Pub. Div.,p.195.

LIST OF PUBLICATIONS RESULTING FROM A.F.O.S.R. SUPPORT

1. R. Fernandez, J.C. Lecomte and T.Z. Kattamis, "Effect of Solidification Parameters on the growth Geometry of MC Carbides in IN-100 Dendritic Monocrystals," Met. Trans. A, Vol. 9A, 1978, p. 1381.
2. T.Z. Kattamis and J.C. Lecomte, "A Novel Method for the Establishment of Solvus Surfaces as Demonstrated with Nickel-Base Alloys," J. Mater. Sci , Vol. 13, 1978, p. 2731.
3. G.D. Merz, T.Z. Kattamis and A.F. Giamei, "Microsegregation and Homogenization of Ni-7.5wt%Al-2.0wt%Ta Dendritic Mono-Crystals," J. Mater. Sci., Vol. 14, 1979, p. 663.
4. T.Z. Kattamis, "Quantitative Metallographic Evaluation of Cast Microstructures," Proceedings of the International Symposium on Quantitative Metallography, Florence, November 21-23, 1978, p.1.
5. P.W. Paterson, T.Z. Kattamis and A.F. Giamei, "Coarsening Kinetics During Solidification of Ni-Al-Ta Dendritic Monocrystals," Met. Trans. A, Vol. 11A, 1980, p. 1059.
6. R. Kadalbal, J.J. Montoya-Cruz and T.Z. Kattamis, "Solute Redistribution During and After Solidification of Ni-Al-Ta Dendritic Monocrystals," Met. Trans. A, Vol. 11A, 1980, p. 1547.
7. R. Kadalbal, J.J. Montoya-Cruz and T.Z. Kattamis, "Solidification Microstructure and Microsegregation of Laser-Glazed Ni-Al-Ta and Ni-Al-Cr Dendritic Monocrystals," Proceedings of the Materials Research Society Symposium, Cambridge, Massachusetts, November 26-30, 1979, Academic Press, Inc., 1980, p. 740.
8. R. Kadalbal, J.J. Montoya-Cruz and T.Z. Kattamis, "Rapid Solidification of Ternary Nickel-Base Alloys", Proceedings of

the 2nd International Conference on Rapid Solidification Processing, Reston, VA, March 1980,"Rapid Solidification Processing, Principles and Technology II,"Claitor's Pub. Div., p. 195.

9. T.Z. Kattamis, "Solidification Microstructure of Laser Processed Alloys and Its Impact on Some Properties", to appear in Proceedings of TMS Conference on "Lasers in Metallurgy," held in Chicago, Ill., February 23, 1981.

10. J.J. Montoya-Cruz, R. Kadalbal, T.Z. Kattamis and A.F. Giamei, "Coarsening and Microsegregation of Ni-Al-Cr Dendritic Monocrystals", submitted for publication, Met. Trans. A.

11. R. Kadalbal and T.Z. Kattamis "Effect of Microalloying with C, B and Zr on the Solidification Microstructure of Ternary Nickel-Base Alloy Dendritic Monocrystals," in preparation.

12. W. Schnake, T.Z. Kattamis and A.F. Giamei "Control of Solidification Microstructure and Microsegregation of B-1900 Dendritic Monocrystals", to be submitted for publication, Met. Trans. A.

13. R. Kadalbal and T.Z. Kattamis, "Effect of Liquid Convection on Microstructural Fineness of Ni-Al-Ta Dendritic Monocrystals" in preparation.

14. T.Z. Kattamis and A.F. Giamei, "Optimized Solidification Microstructure and Minimized Microsegregation in Nickel-Base Dendritic Monocrystals", to be prepared and presented at the next Seven Springs, PA Conference on Nickel Superalloys.

LIST OF PERSONNEL

April 1,1977-March 31,1978

University of Connecticut

1. T.Z.Kattamis,Professor,Principal Investigator
2. G.D.Merz,Graduate Assistant, Ph.D.candidate
3. P.Kunz,Research Aide

Pratt & Whitney Aircraft

1. A.F.Giamei,Senior Staff Scientist
2. W.F.Gustafson,Technician

April 1,1978-March 31,1979

University of Connecticut

1. T.Z.Kattamis,Professor,Principal Investigator
2. R.Kadalbal,Graduate Assistant, M.S.candidate (7 months)
3. G.D.Merz,Graduate Assistant,Ph.D. candidate (9 months)
4. J.J.Montoya-Cruz,Graduate Student,M.S. candidate
5. P.W.Peterson,Part-time Graduate Student,M.S.candidate
6. P.Kunz,Research Aide

Pratt & Whitney Aircraft

1. A.F.Giamei,Senior Staff Scientist
2. W.F.Gustafson,Technician

April 1,1979-March 31,1980

University of Connecticut

1. T.Z.Kattamis,Professor,Principal Investigator
2. B. Dukiet-Zawadzka,Post-doctoral fellow,Summer 1979
3. R.Kadalbal,Graduate Assistant,M.S.candidate
4. J.J.Montoya-Cruz,Graduate Assistant,M.S.candidate
5. R.Bekech,Graduate Assistant,M.S.candidate

Pratt & Whitney Aircraft

1. A.F.Giamei,Senior Staff Scientist

April 1,1980-August 31,1981

University of Connecticut

1. T.Z.Kattamis,Professor,Principal Investigator
2. R.Kadalbal,Graduate Assistant,Ph.D.candidate
3. W.Schnake,Graduate Assistant,M.S.candidate
4. R.Bekech,Graduate Assistant,M.S.candidate (5 months)
5. J.Piotrowski,Graduate Assistant,M.S.candidate (6 months)

Pratt & Whitney Aircraft
(United Technologies Research Laboratories)

1. A.F.Giamei,Senior Staff Scientist.

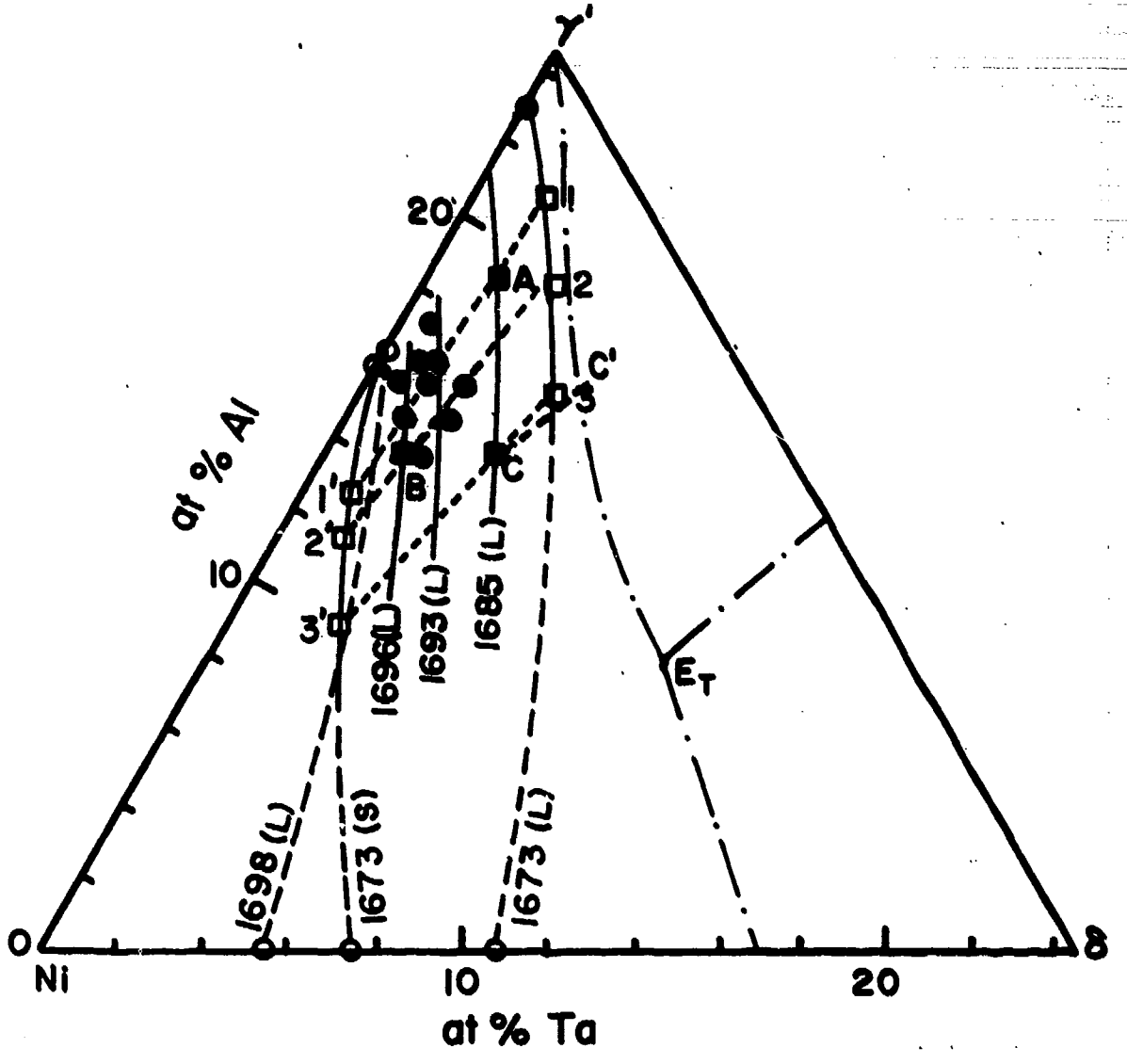

Fig. 1: Basal projection of the nickel-rich corner of the Ni-Al-Ta phase diagram.

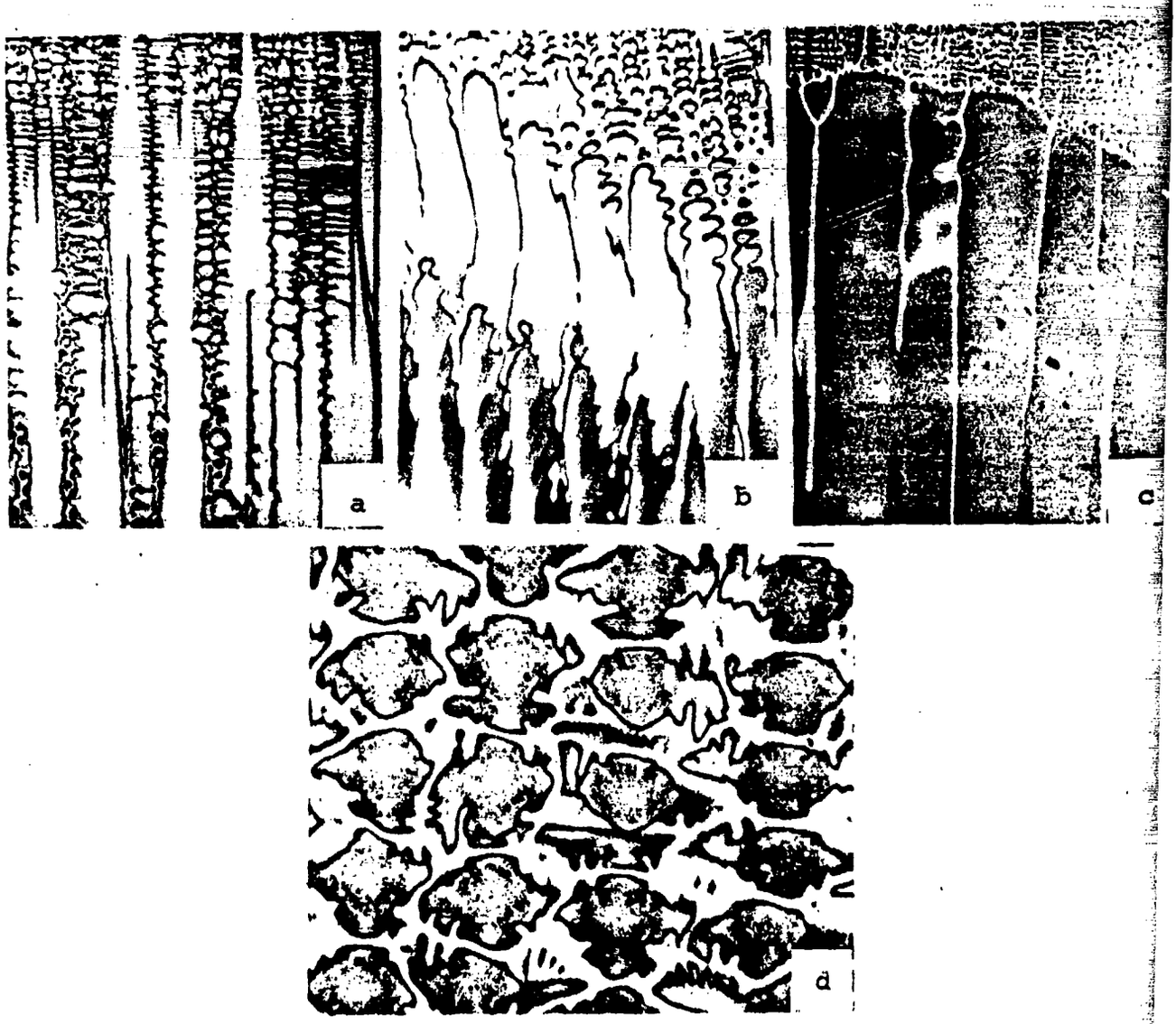

Fig. 2: Photomicrographs of longitudinal sections of Ni-13.4at%Al-1.8at%Ta dendritic monocrystals continuously grown at 0.2 m/h and coarsened for: (a) 0 s,(b) 10 s and (c) 90 s, prior to quenching the remaining liquid, 50X,(d) photomicrograph of a transverse section of specimen (a) corresponding to 1673K,100X.

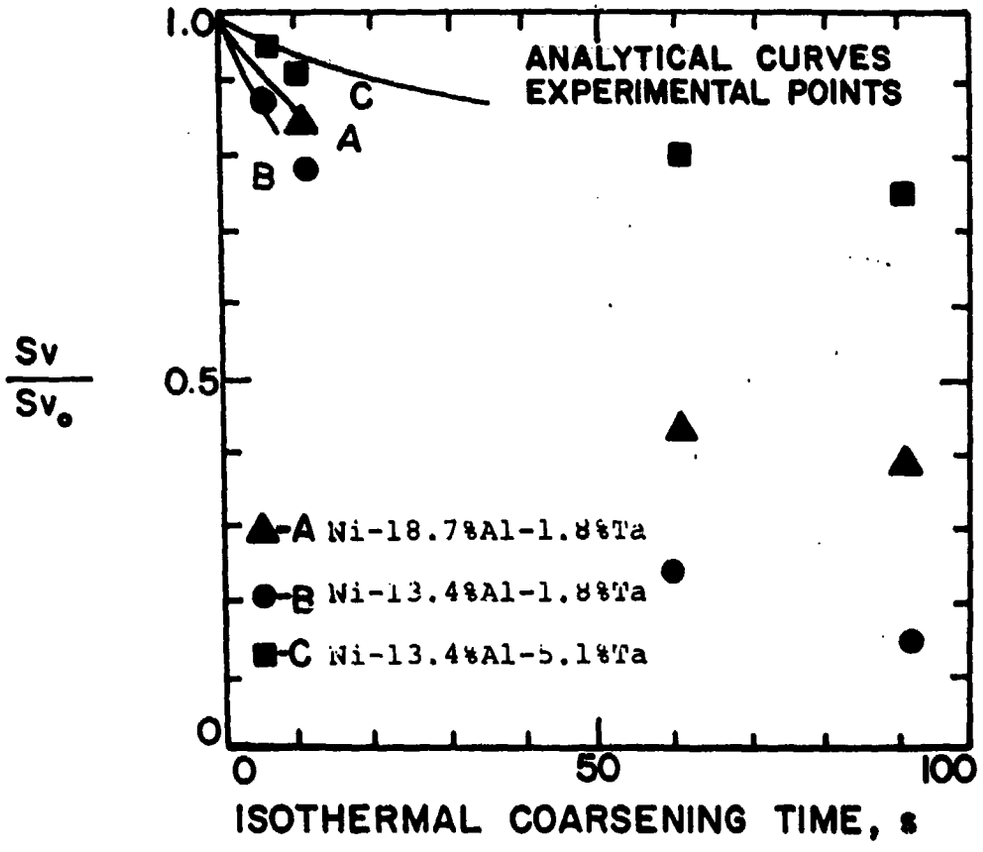

Fig. 3: Variation of S_v/S_{v_o} versus isothermal coarsening time composition. Analytical curves and experimenta points for dendritic monocrystals.

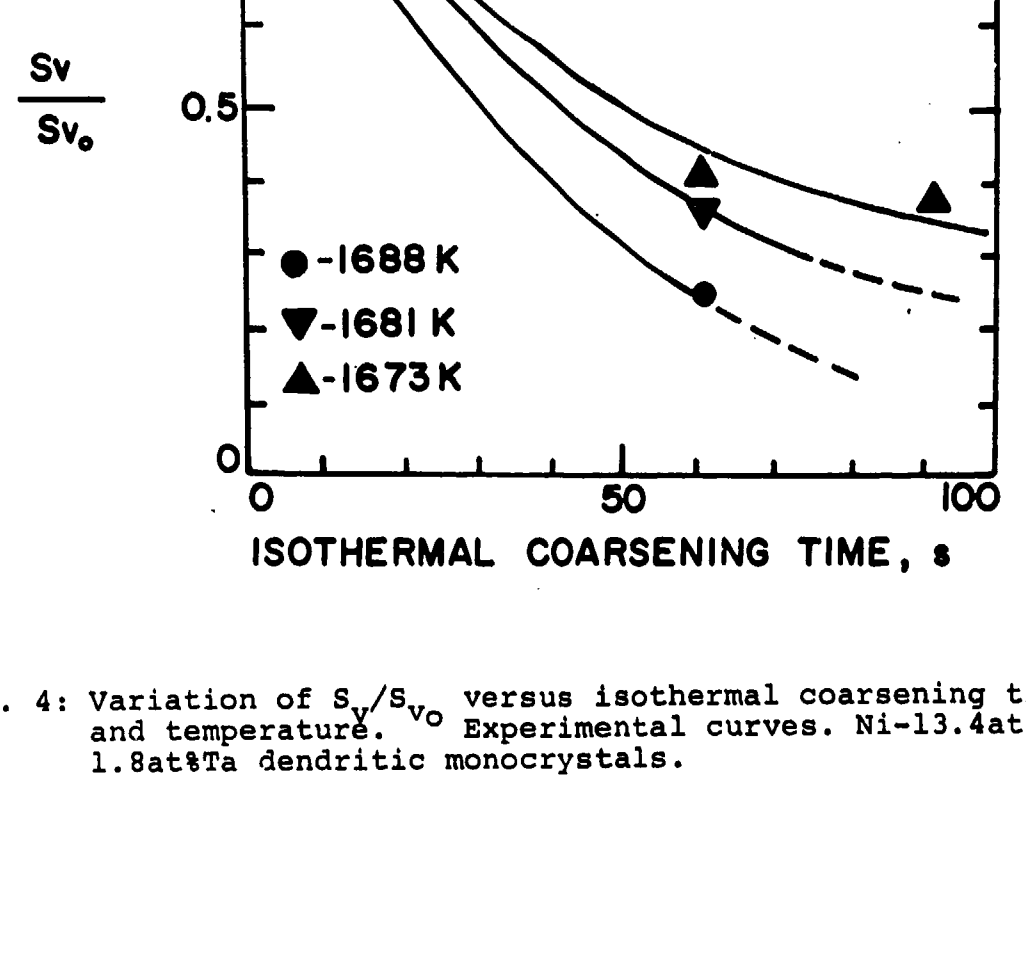

Fig. 4: Variation of S_v/S_{vo} versus isothermal coarsening time and temperature. Experimental curves. Ni-13.4at%Al-1.8at%Ta dendritic monocrystals.

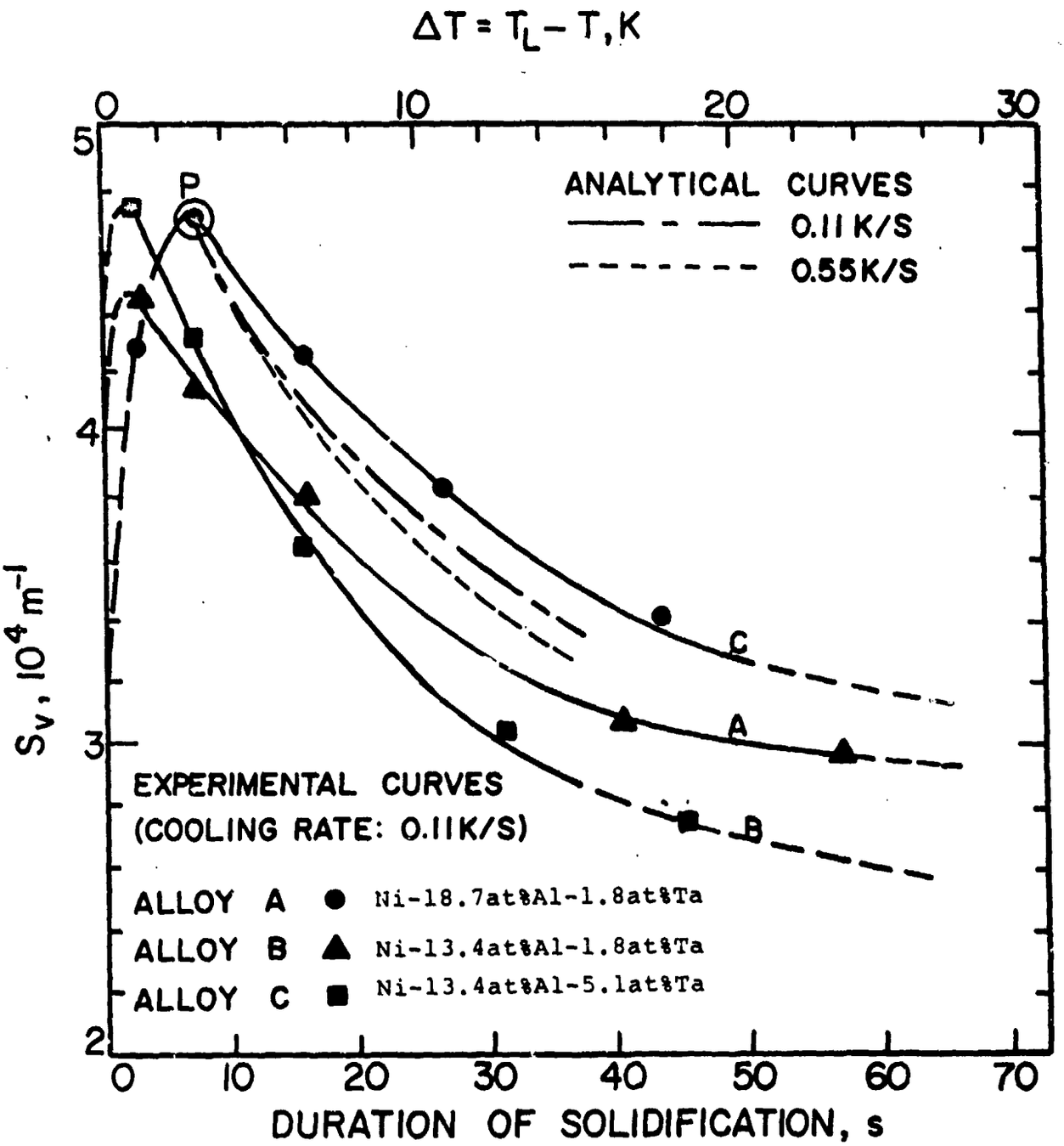

Fig. 5: Variation of S_v versus duration of solidification or temperature difference from the liquidus. Experimental curves for alloys A, B and C, and for a cooling rate of 0.11K/s. Analytical curves for alloy C and for cooling rates of 0.11 and 0.55K/s.

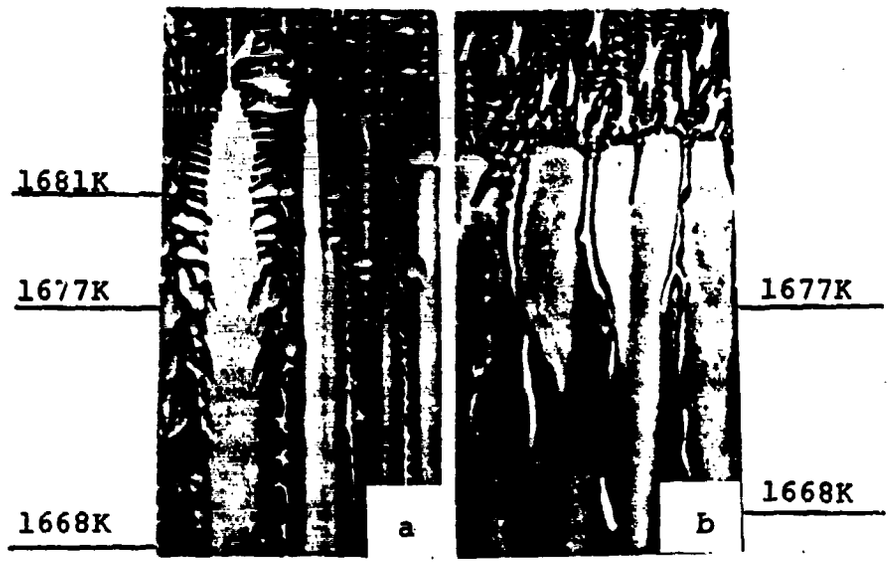

Fig. 6: Longitudinal sections of Ni-13.lat%Al-5.lat%Ta dendritic monocrystals,50X. (a) specimen grown at 0.25m/h under a gradient of 8×10^3 K/m prior to quenching, (b) specimen grown under the same conditions and coarsened for 3 min prior to quenching.

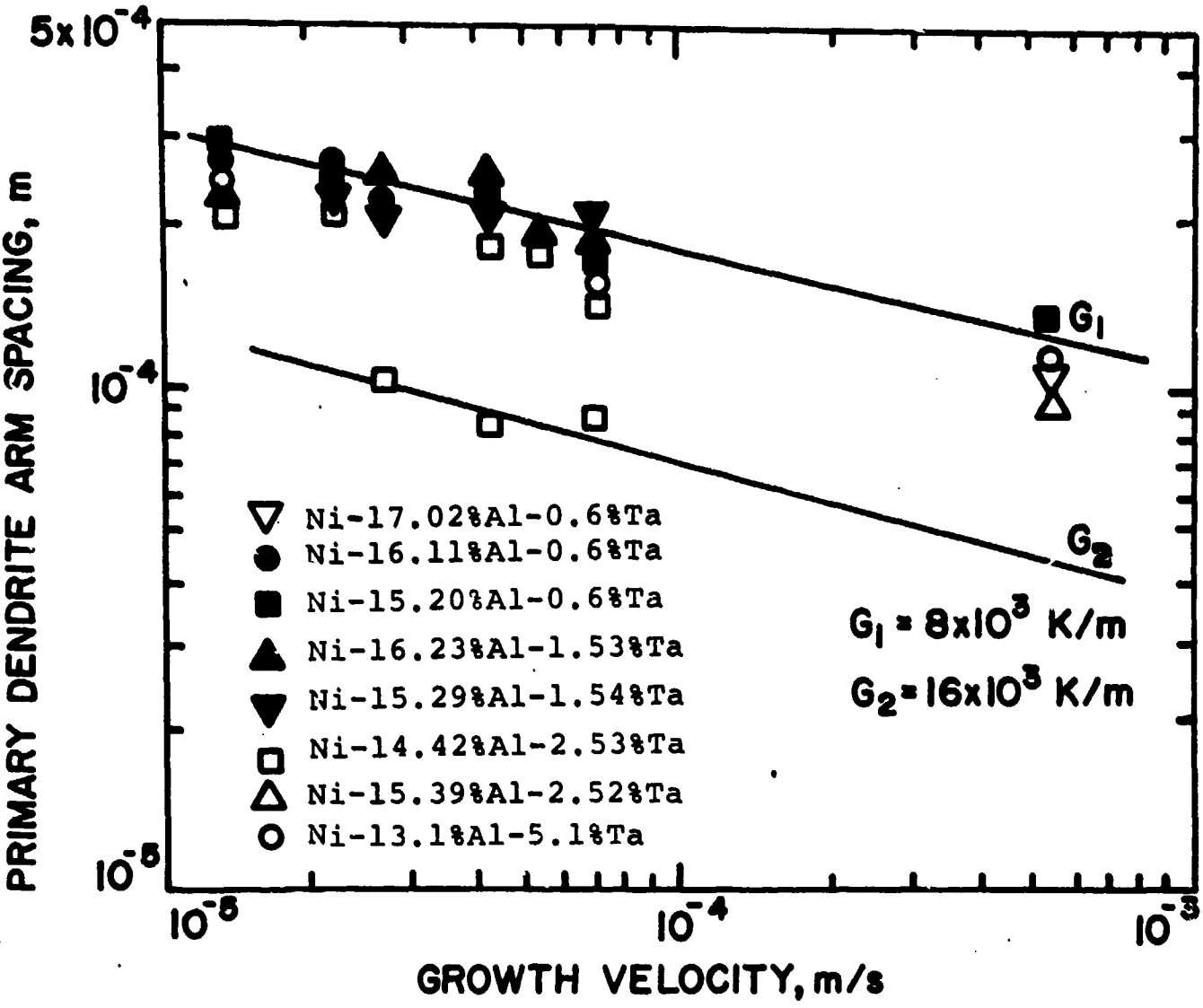

Fig. 7: Primary dendrite arm spacing versus growth velocity for various Ni-Al-Ta alloy compositions and two different temperature gradients.

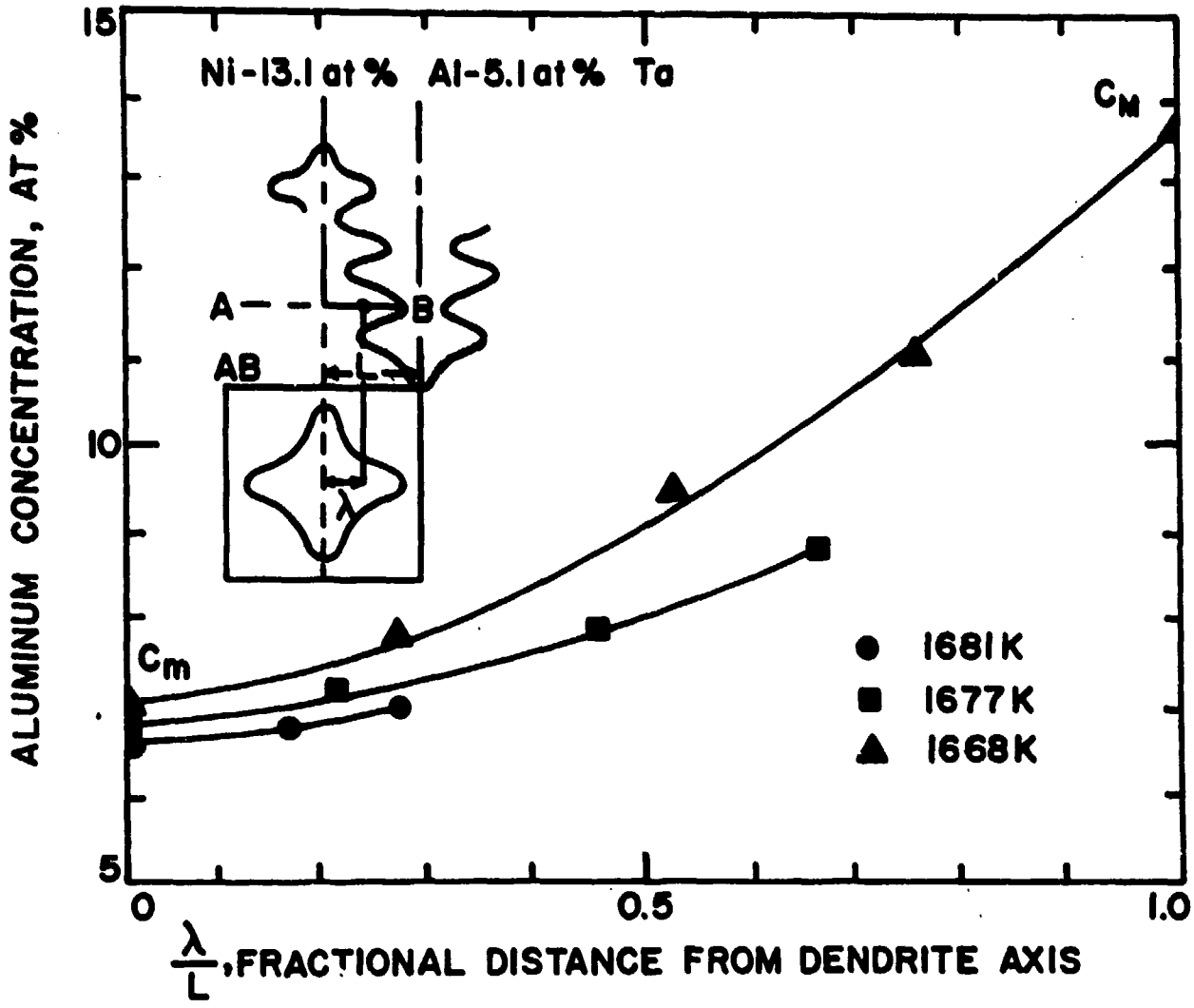

Fig.8 : Aluminum concentration versus fractional distance from the dendrite axis at 1681,1677 and 1688K. Ni-13.1at%Al-5.1at%Ta.

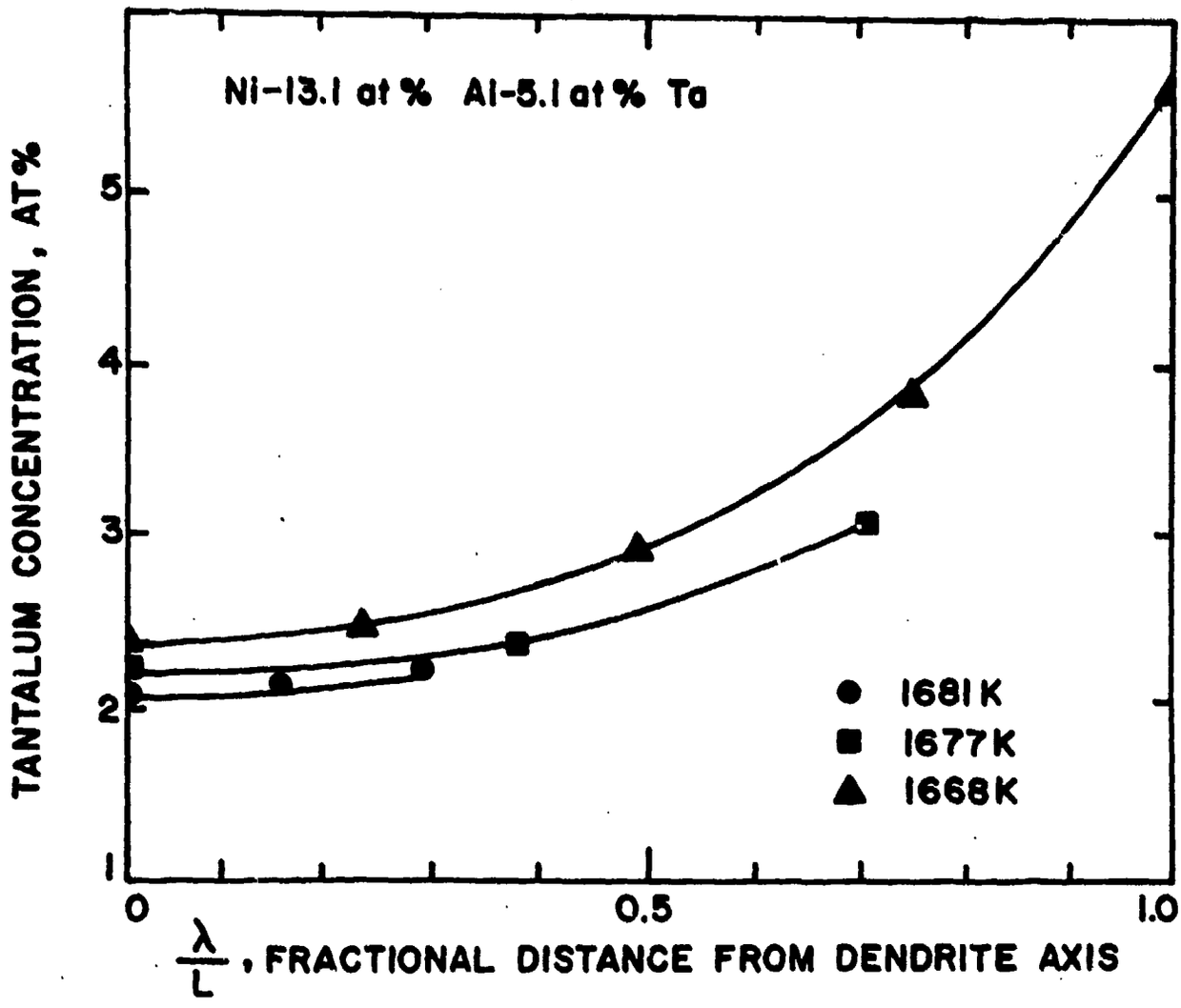

Fig. 9 ; Tantalum concentration versus fractional distance from the dendrite axis at 1681,1677 and 1668K. Ni-13.1at%Al-5.1at%Ta.

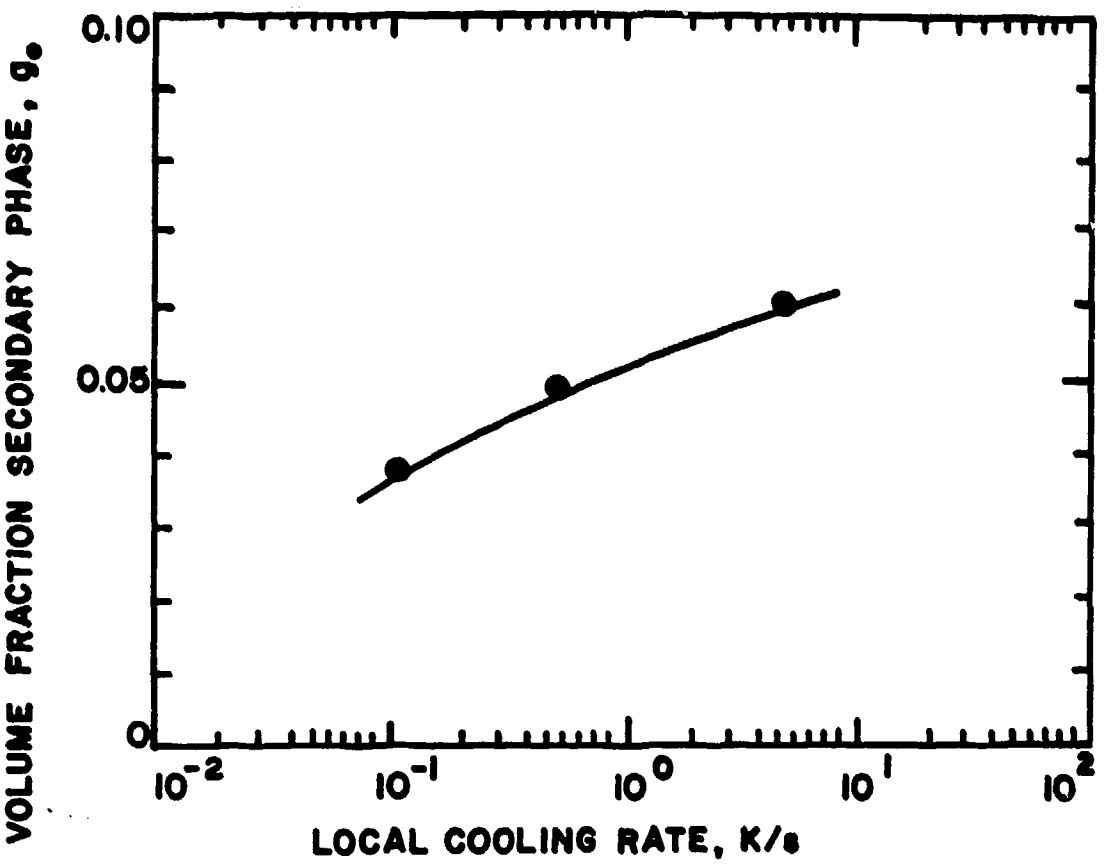

Fig. 10 :Volume fraction of interdendritic nonequilibrium γ' phase, g_o, versus local cooling rate. Ni-13.lat%Al-5.lat%Ta.

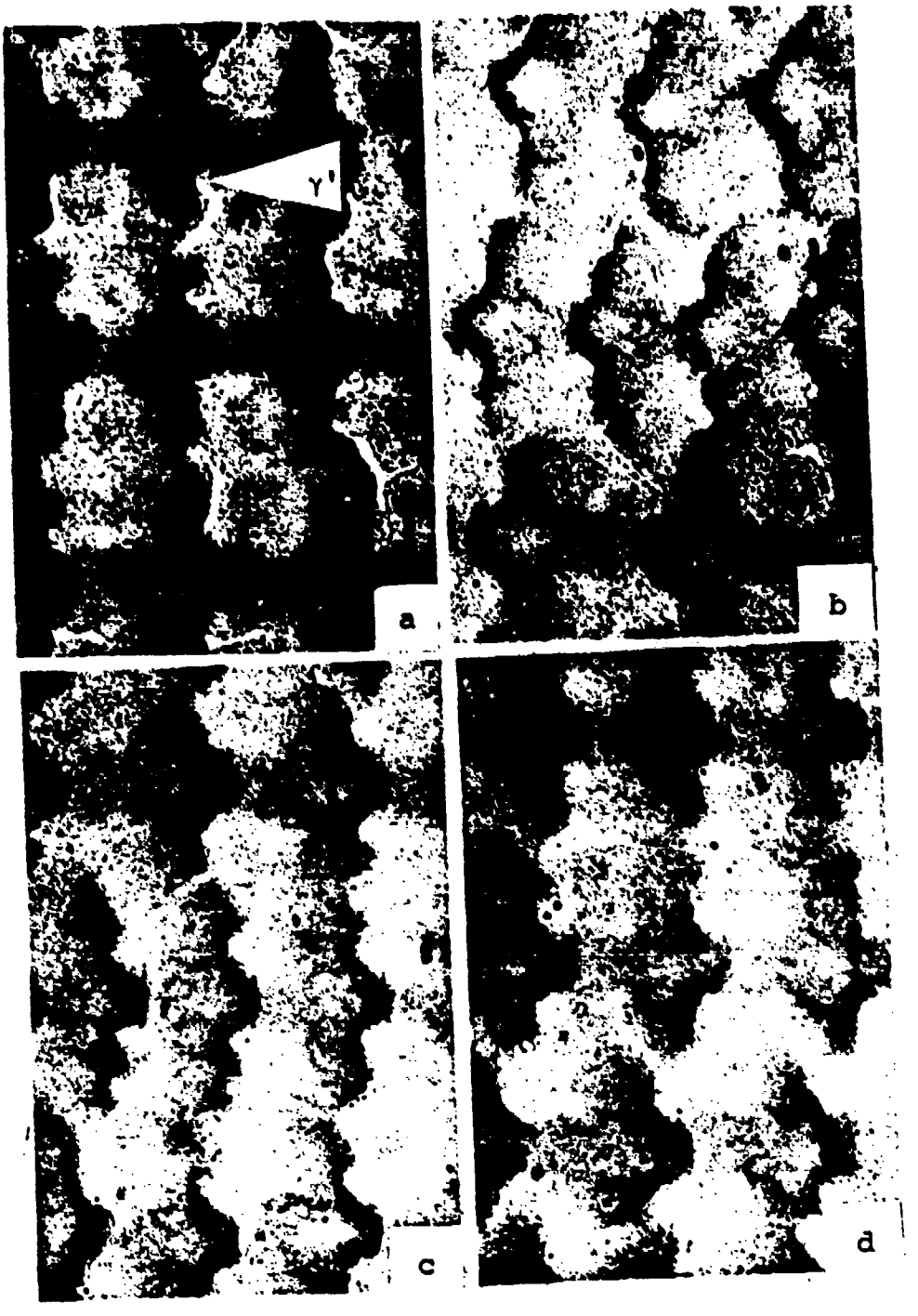

Fig. 11: Photomicrographs of transverse sections of dendritic monocrystals of Ni-13.1at%Al-5.1at%Ta taken at different distances below the eutectic isotherm, 100X. The corresponding temperatures are: (a) 1668K, (b) 1655.8K, (c) 1651.5K and (d) 1642K.

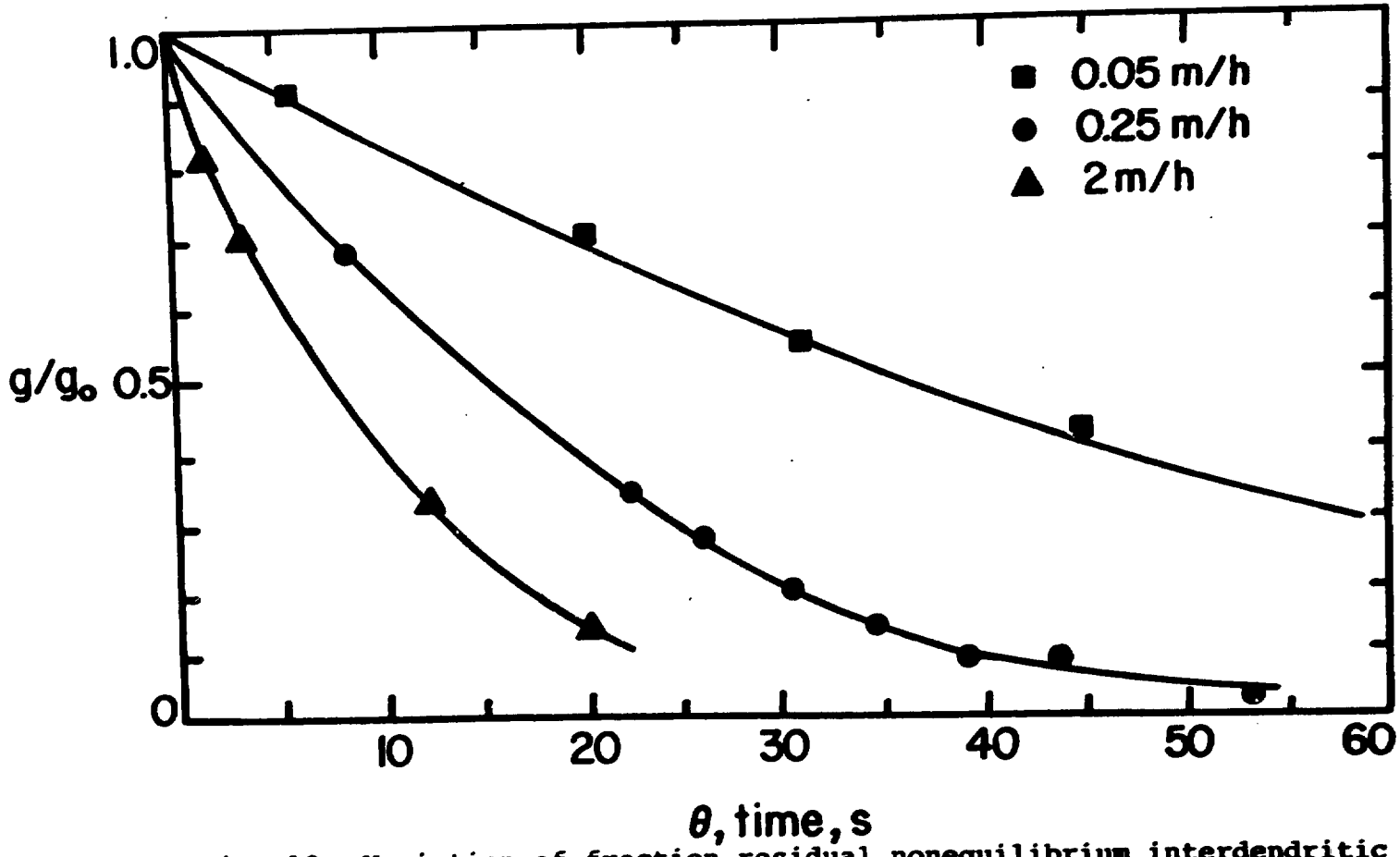

Fig. 12 : Variation of fraction residual nonequilibrium interdendritic γ' versus time during monocrystal pulling. Zero time corresponds to the eutectic isotherm. Pulling rates are: 0.05,0.25 and 2 m/h. Ni-13.1at%Al-5.1at%Ta.

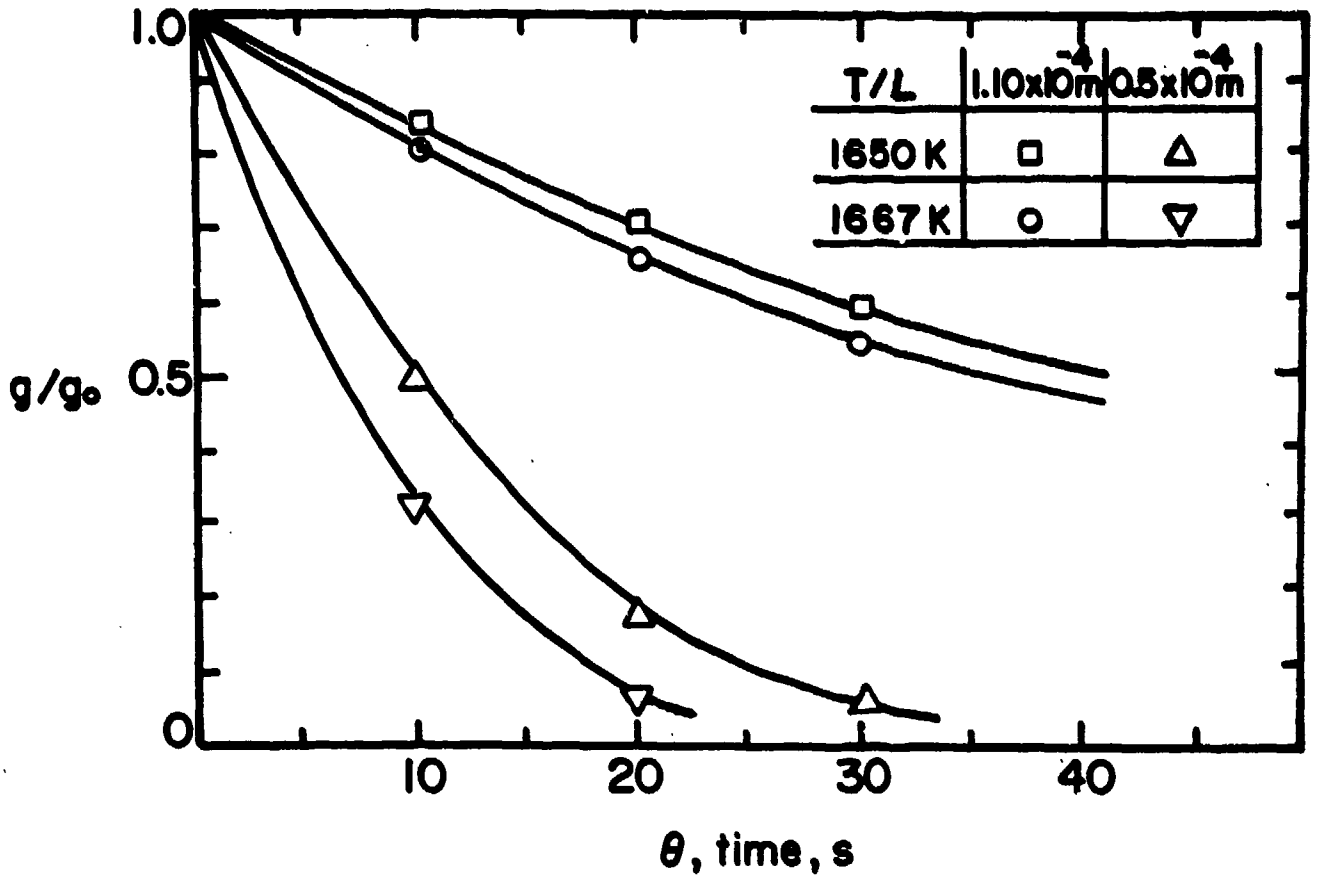

Fig. 13: Variation of fraction residual nonequilibrium interdendritic phase γ' with isothermal holding time, for two temperatures: 1650 and 1667K and two microstructures of primary dendrite arm spacings: $2x1.10x10^{-4}$m and $2x0.5x10^{-4}$m. Ni-13.1 at%Al-5.1at%Ta.

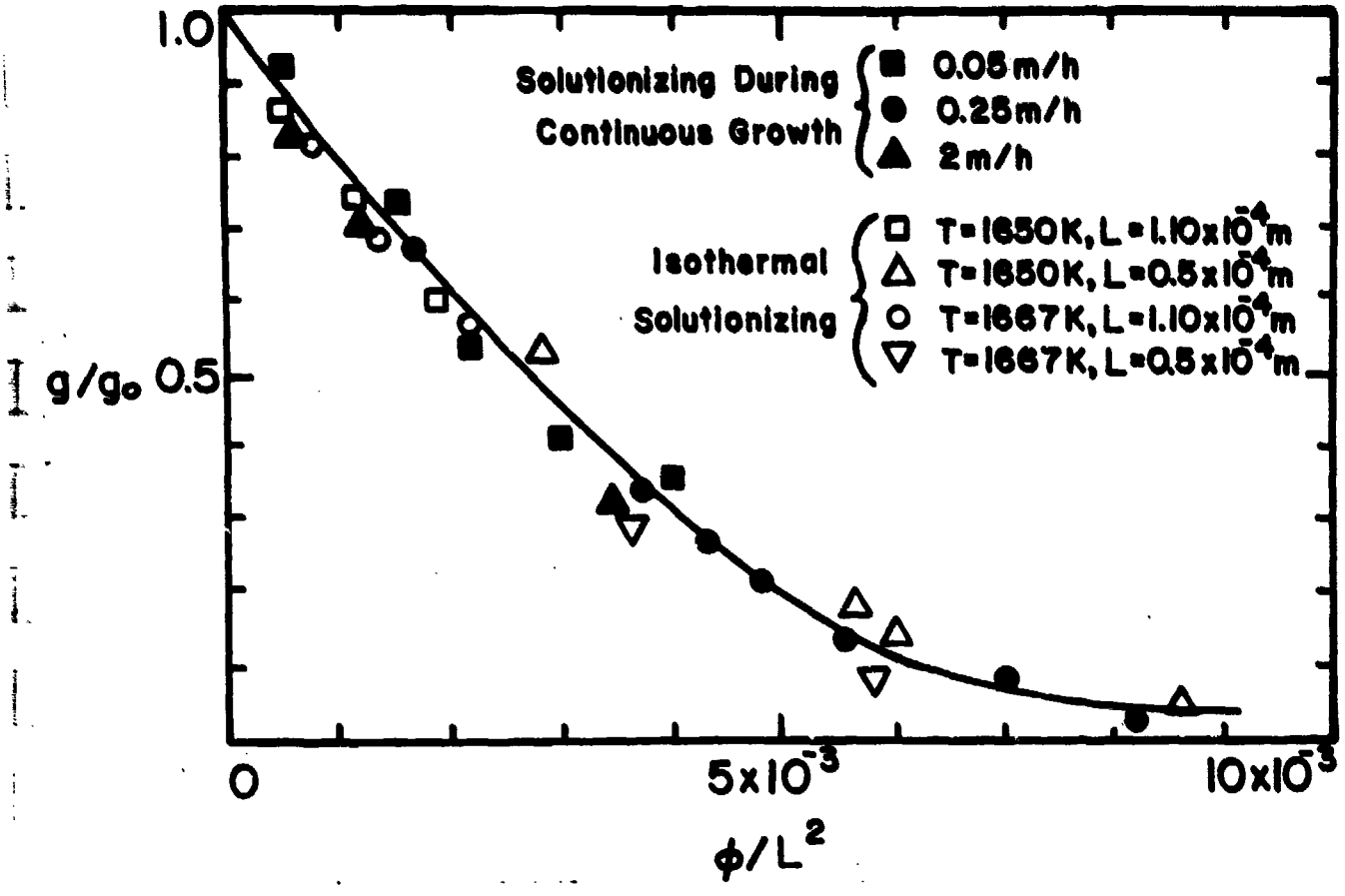

Fig. 14: Variation of g/g_o versus ϕ/L^2 for isothermally solutionized specimens and specimens that were solutionized during continuous growth. Ni-13.lat%Al-5.lat%Ta.

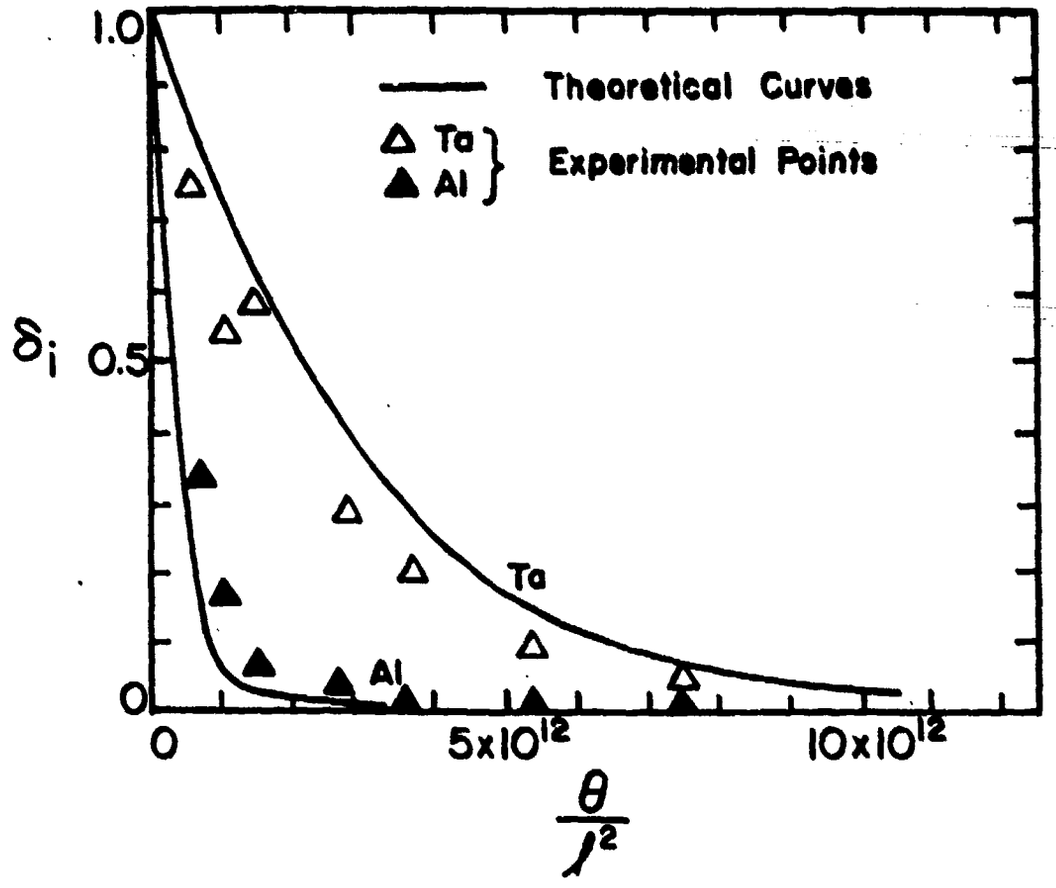

Fig. 15: Index of residual segregation, δ_i, versus θ/l^2 for aluminum and tantalum. Ni-17.5wt%Al-2.0wt%Ta dendritic monocrystals.

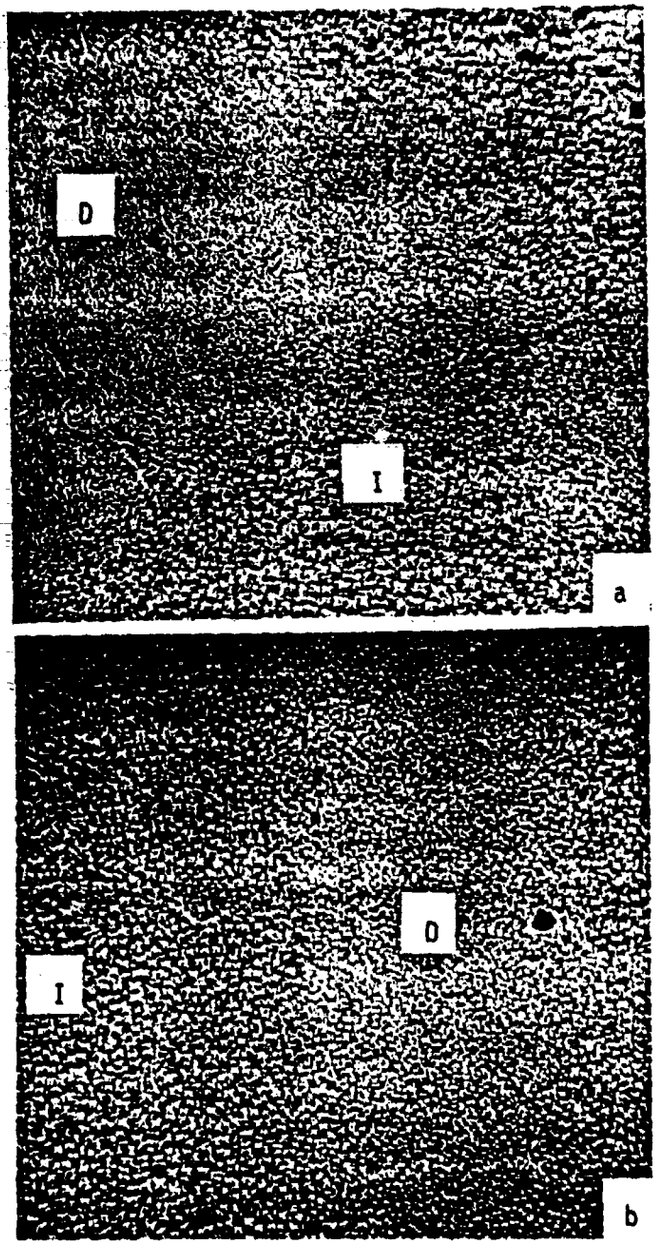

Fig. 16 : Scanning electron micrographs of a transverse section (a) and a longitudinal section (b),1000X. Ni-7.5%Al-2.0%Ta dendritic monocrystal grown at 0.25m/h under a gradient of 16×10^3 K/m. D=dendrite center,I=interdendritic space.

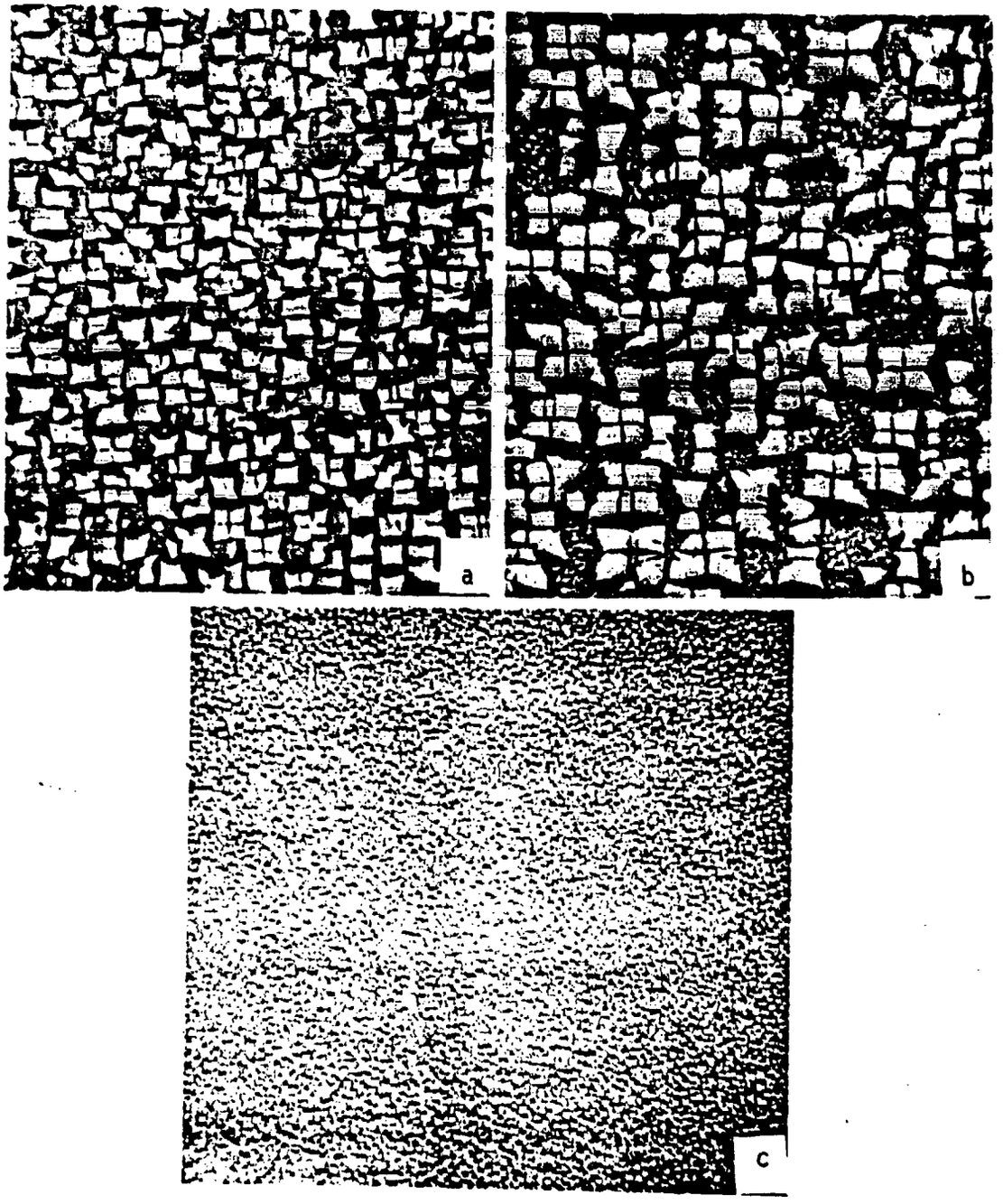

Fig. 17 :Scanning electron micrographs of a longitudinal section of a Ni-7.5%Al-2.0%Ta dendritic monocrystal solidified at 0.25m/h under a gradient of 16×10^3K/m. (a) Center of dendrite,5000X,(b) interdendritic region,5000X. (c) Homogenized specimen,1000X.

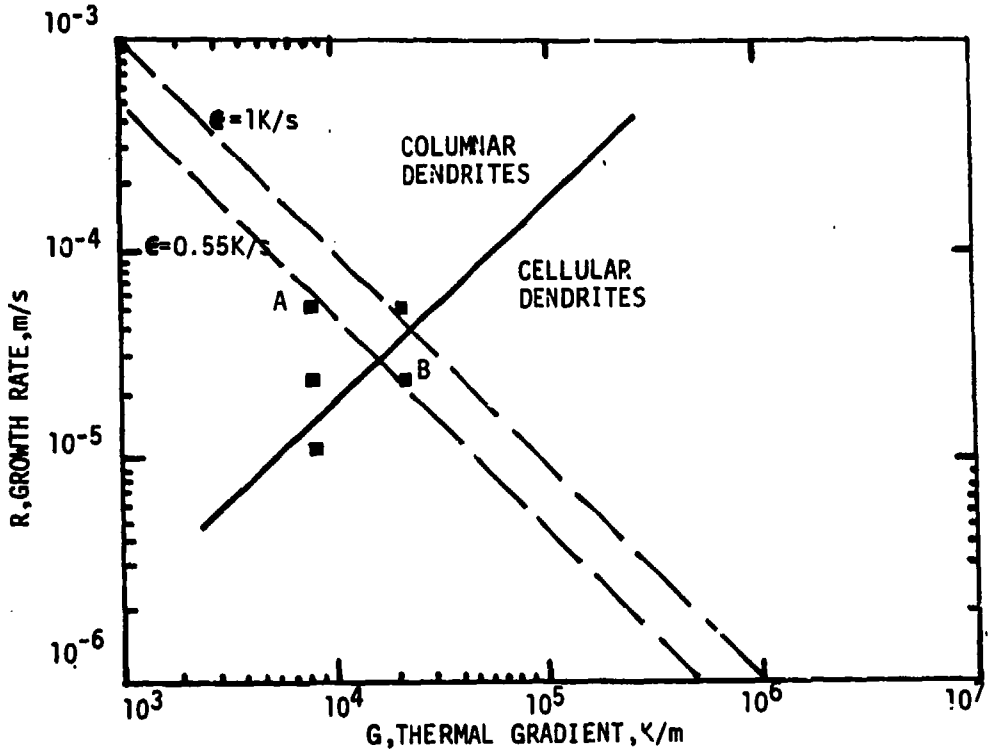

Fig. 18: G-R-ε diagram indicating morphological transition in Ni-18.0at%Al-4.1at%Cr alloy.

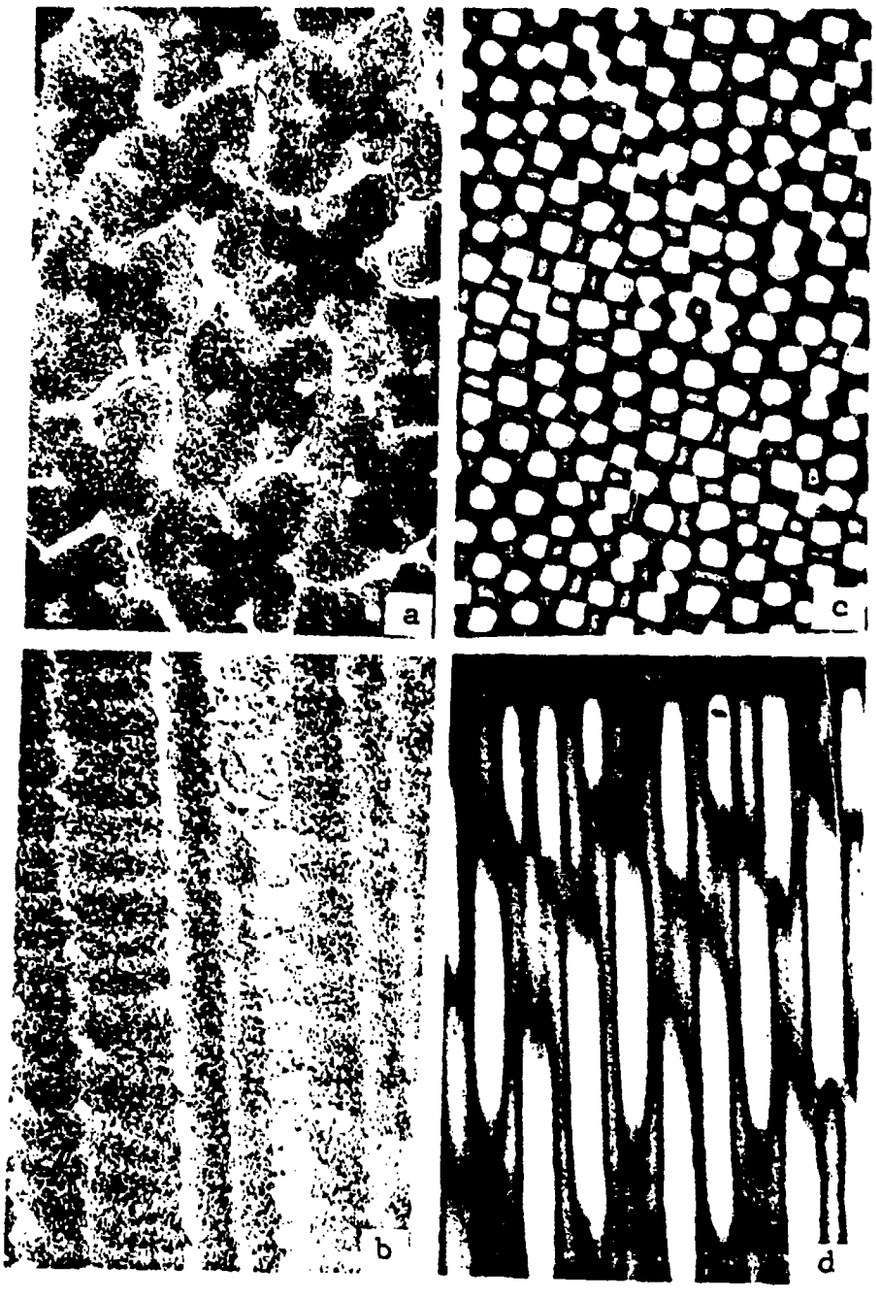

Fig. 19 Photomicrographs of sections of two dendritic monocrystals, A and B, of Ni-18.0at%Al-4.1at%Cr alloy, 55X. (a) and (b) are transverse and longitudinal sections, respectively, of crystal A. $G=8\times10^{3}$K/m, R=0.25m/h. (c) and (d) are transverse and longitudinal sections, respectively, of crystal B. $G=20\times10^{3}$K/m, R=0.10m/h

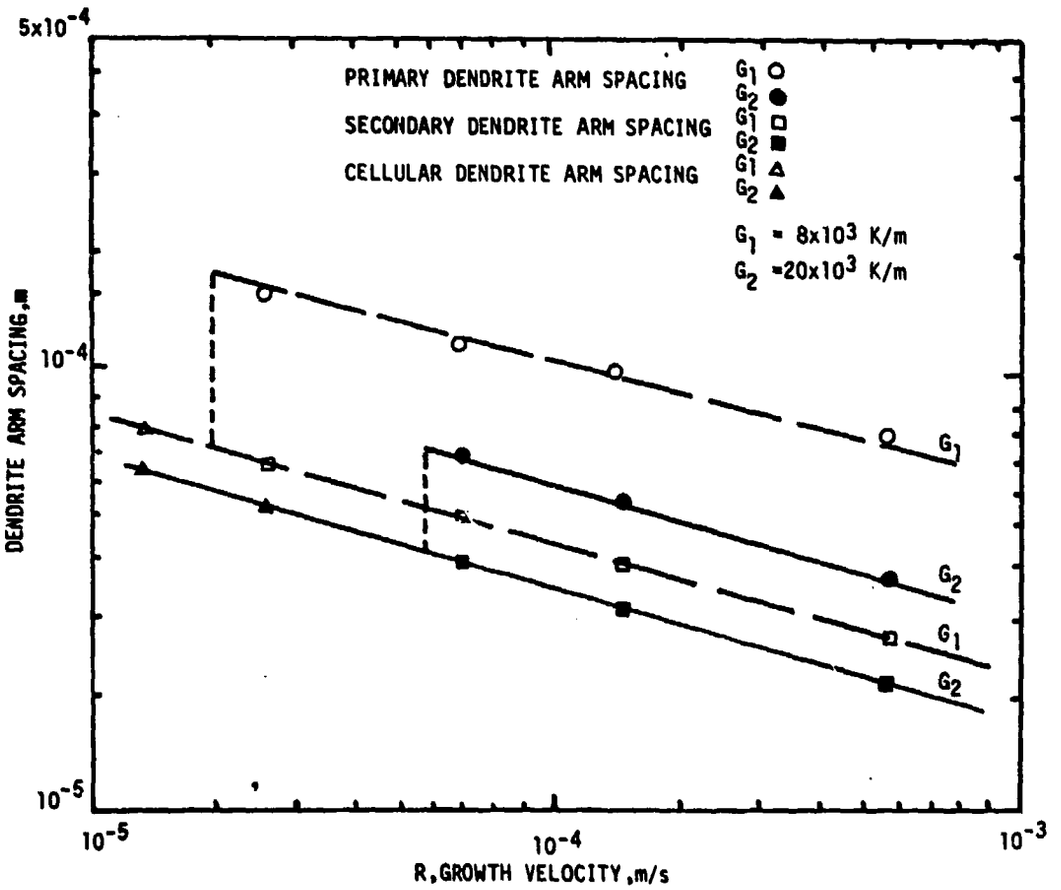

Fig.20: Primary and secondary dendrite arm spacings and cellular dendritic spacing versus growth rate for $G_1=8x10^3$ and $G_2=20x10^3$ K/m. Ni-18.0at%Al-4.1at%Cr alloy. Tthe cellular/columnar transition occurs at $G_2/R_2=G_1/R_1$.

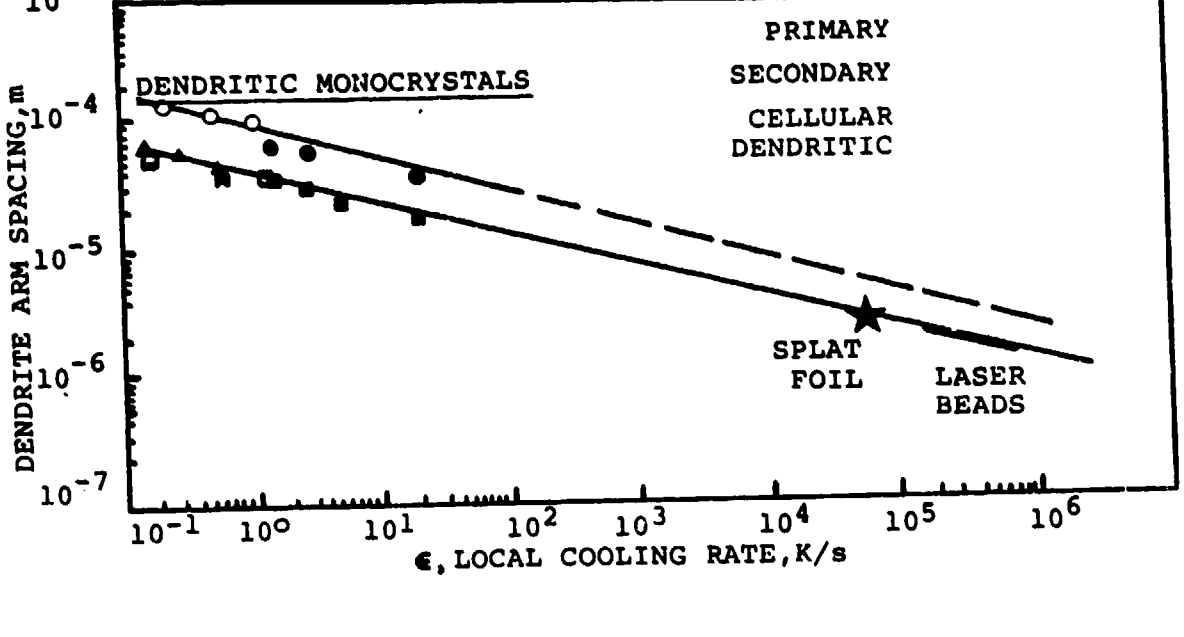

Fig. 21: Primary, secondary and cellular dendritic spacings versus local cooling rate. Ni-18.0at%Al-4.1at%Cr alloy.

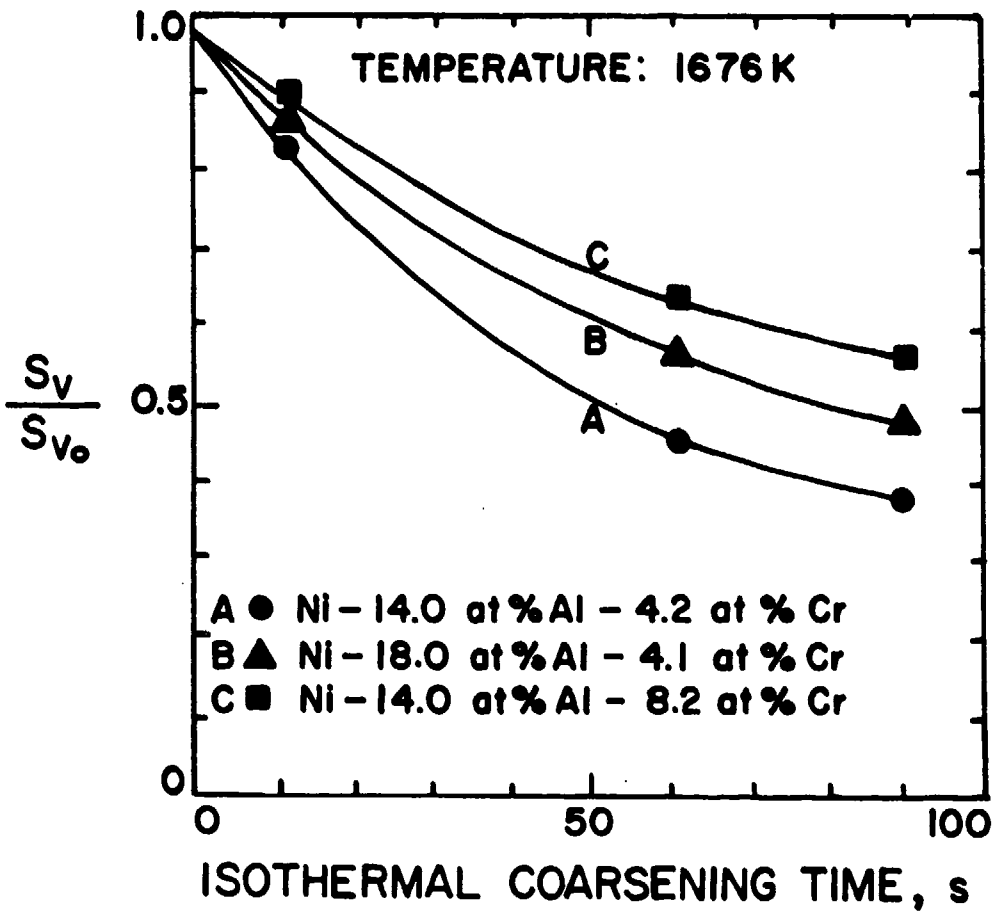

Fig. 22 : Variation of S_V/S_{VO} versus isothermal coarsening time at 1676K and composition. Experimental curves.

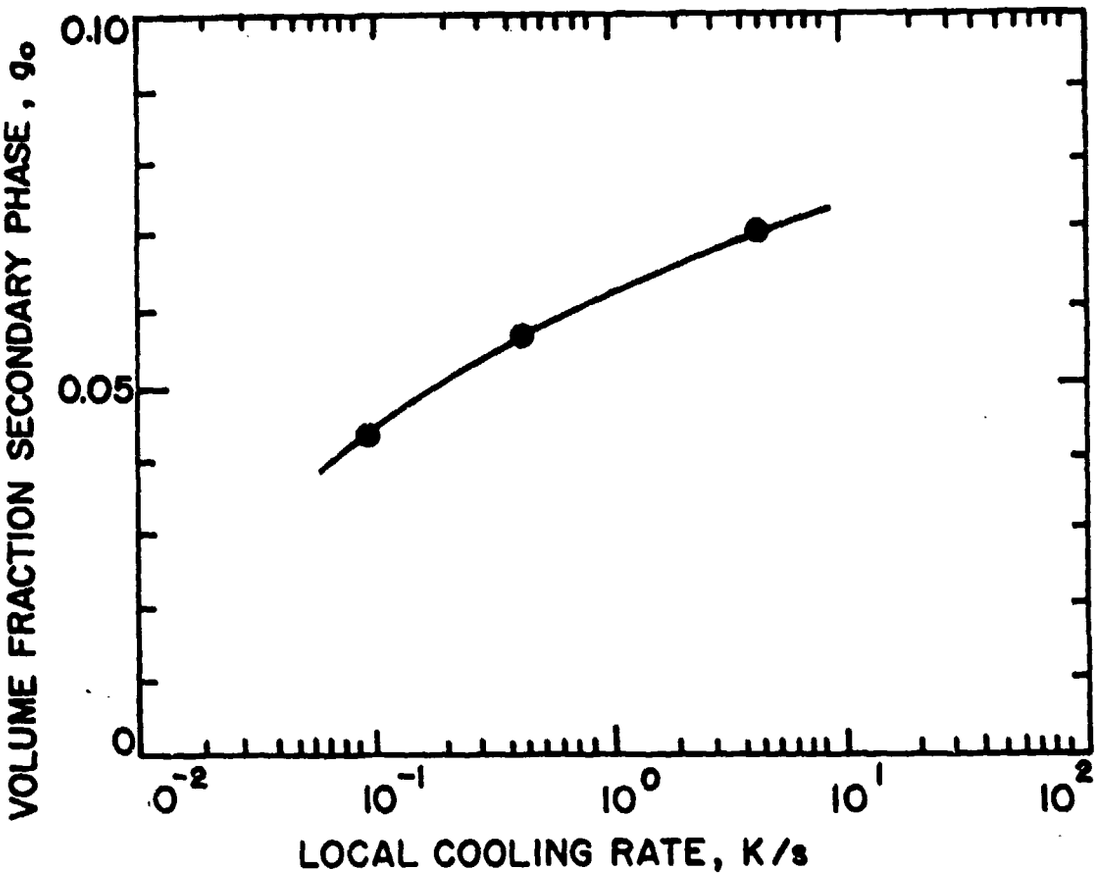

Fig. 23: Volume fraction of interdendritic γ' phase, g_o, versus local cooling rate. Ni-19.2at%Al-11.9at%Cr.

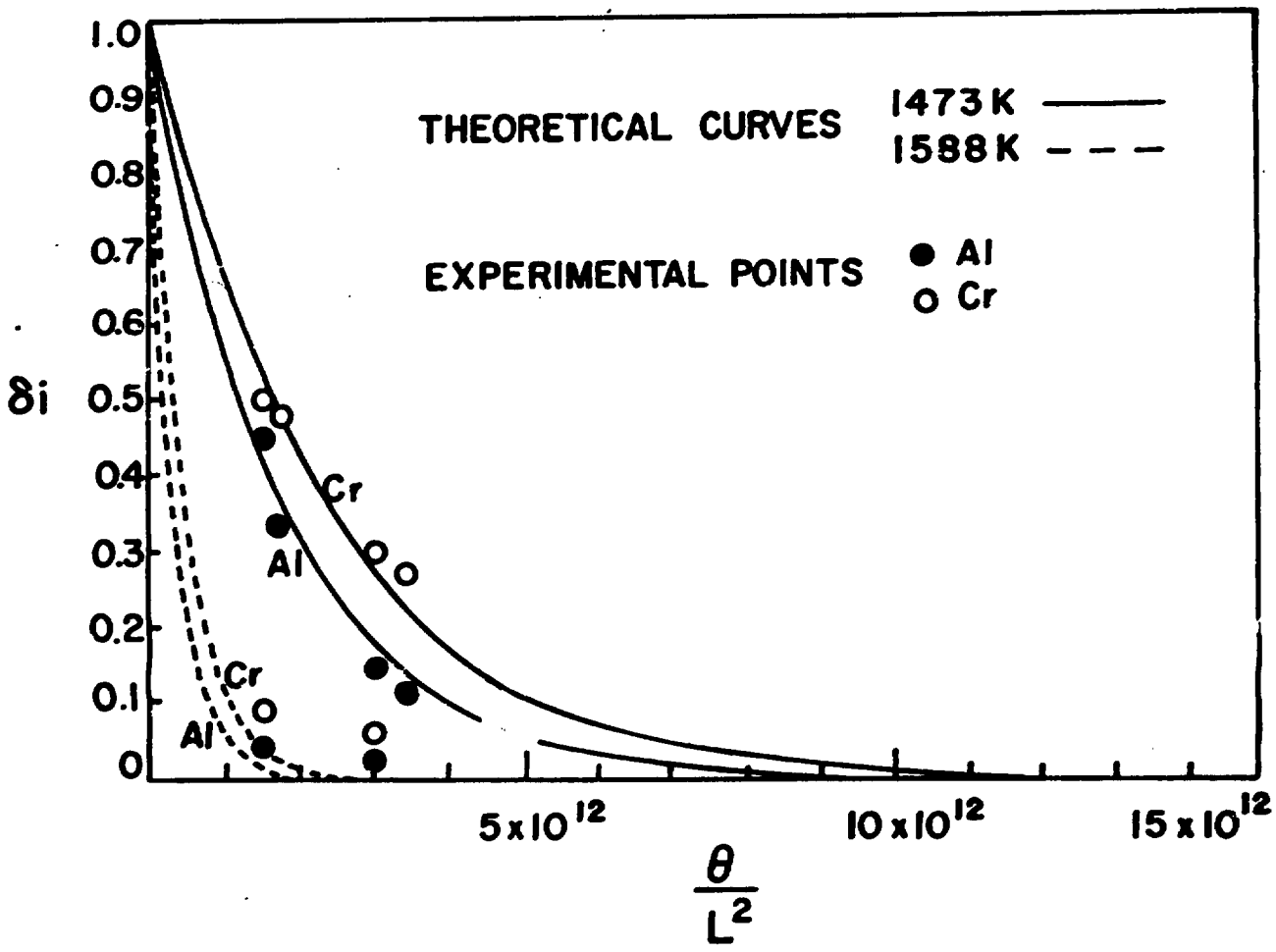

Fig. 24 : Index of residual segregation, δ_i, versus homogenization parameter, t/L^2, for aluminum and chromium. Ni-14.8at%Al-8.2at%Cr dendritic monocrystals.

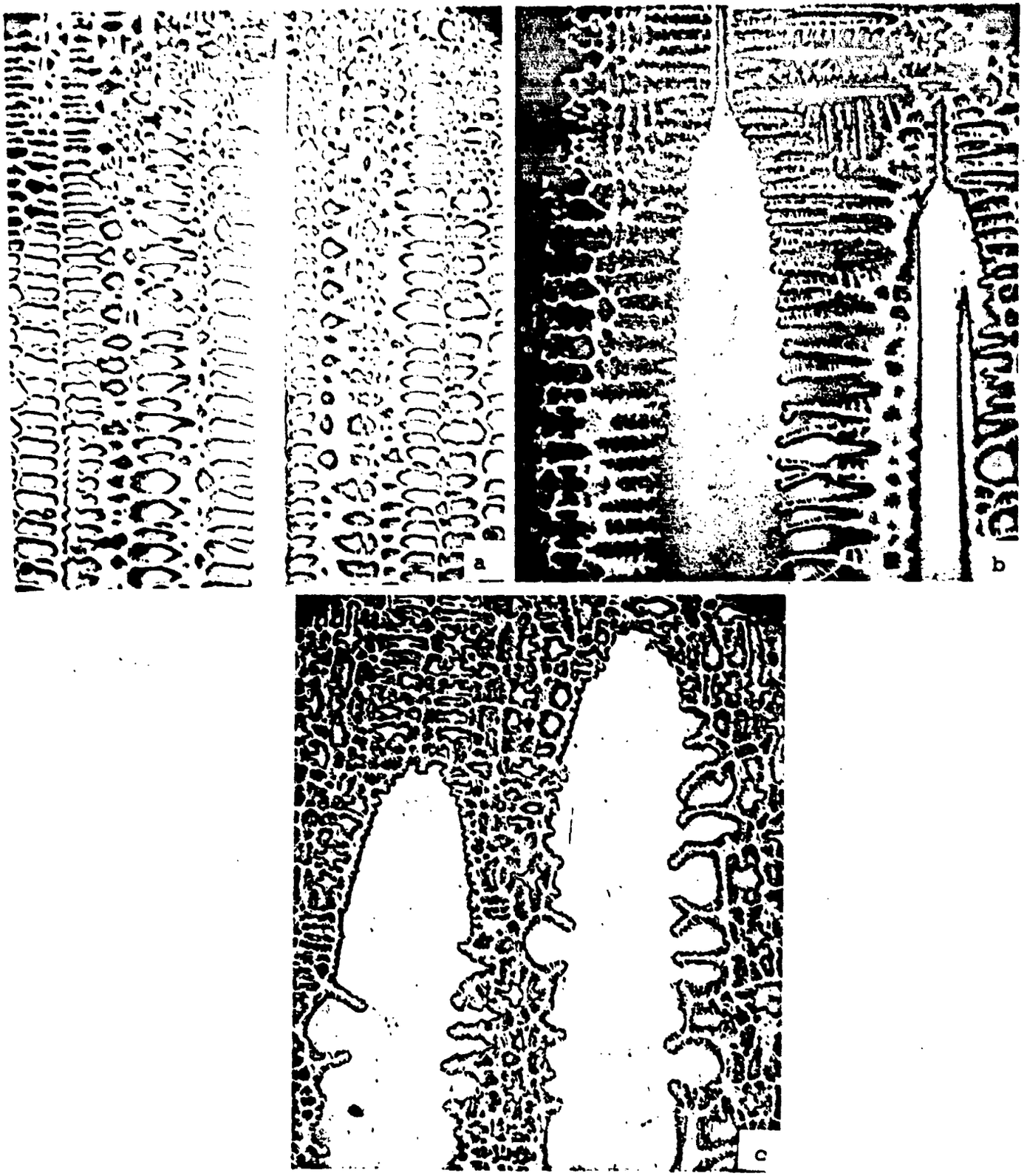

Fig. 25: Photomicrographs of longitudinal sections of dendritic monocrystals of Ni-9.0wt%Al-4.0wt%Cr-1wt%Zr pulled at 25cm/h under a $G=8x10^3$ K/m and coarsened for:(a) 0 s,(b) 1 min and (c) 2.5 min. prior to quenching the remaining liquid.

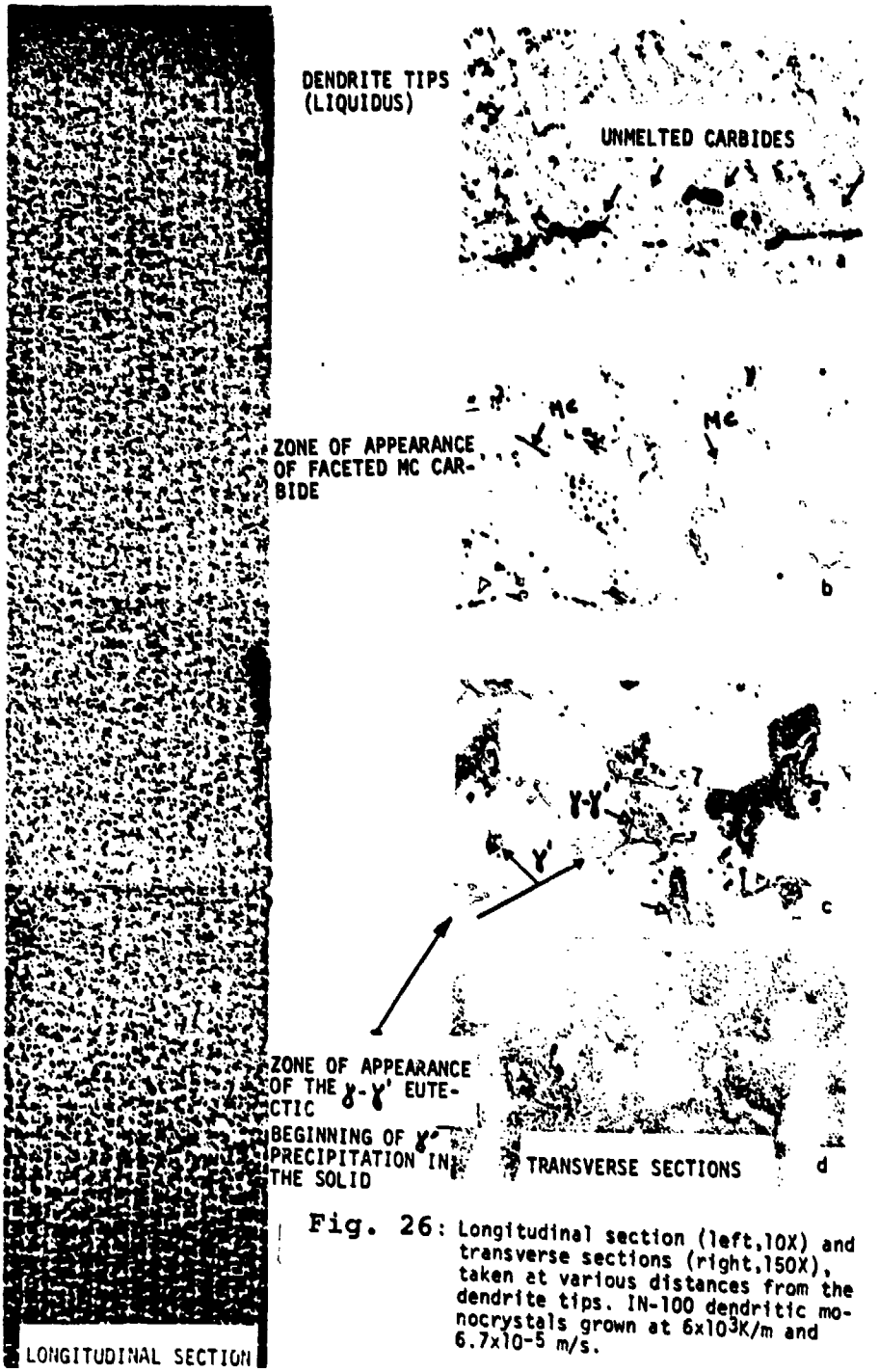

Fig. 26: Longitudinal section (left,10X) and transverse sections (right,150X), taken at various distances from the dendrite tips. IN-100 dendritic monocrystals grown at 6×10^3K/m and 6.7x10-5 m/s.

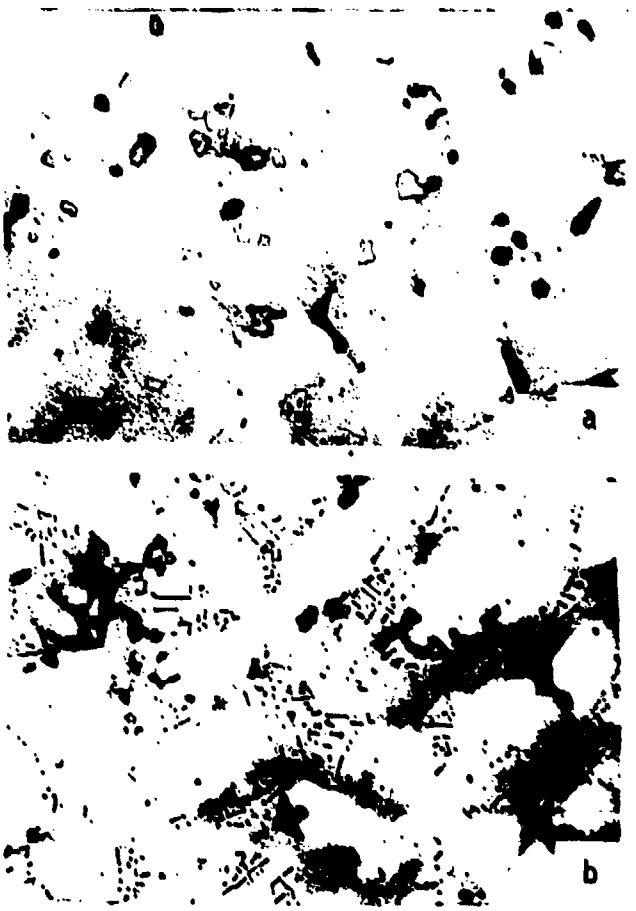

Fig. 27: Faceted carbide (a) and chinese script-type carbide (b) in IN-100 dendritic monocrystals,100X. Sections taken at about 5 K below the eutectic temperature.

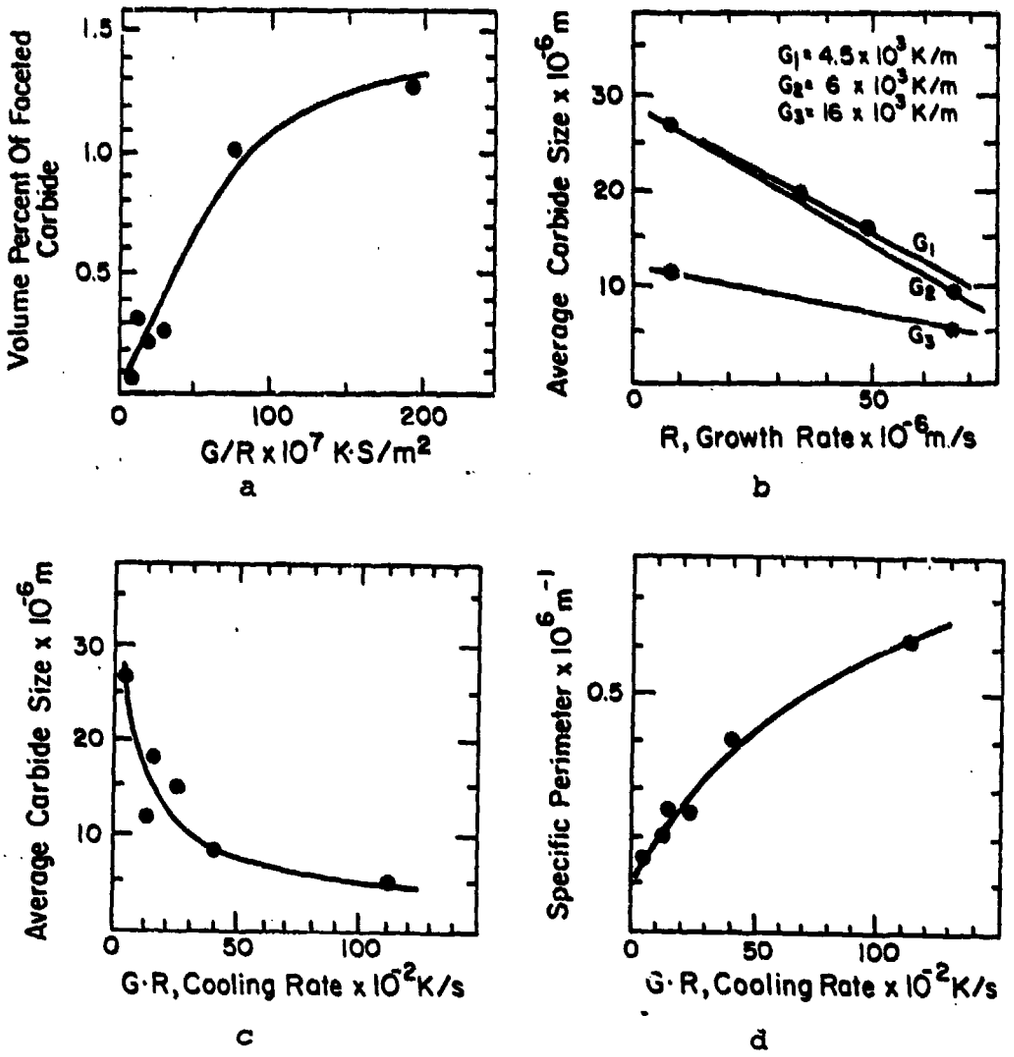

Fig. 28: (a) Volume pct of faceted carbide versus G/R ratio, (b) and (c) average faceted carbide size versus growth rate for three different gradients and versus cooling rate, respectively, and (d) specific perimeter of faceted carbides versus cooling rate. IN-100 dendritic monocrystals.

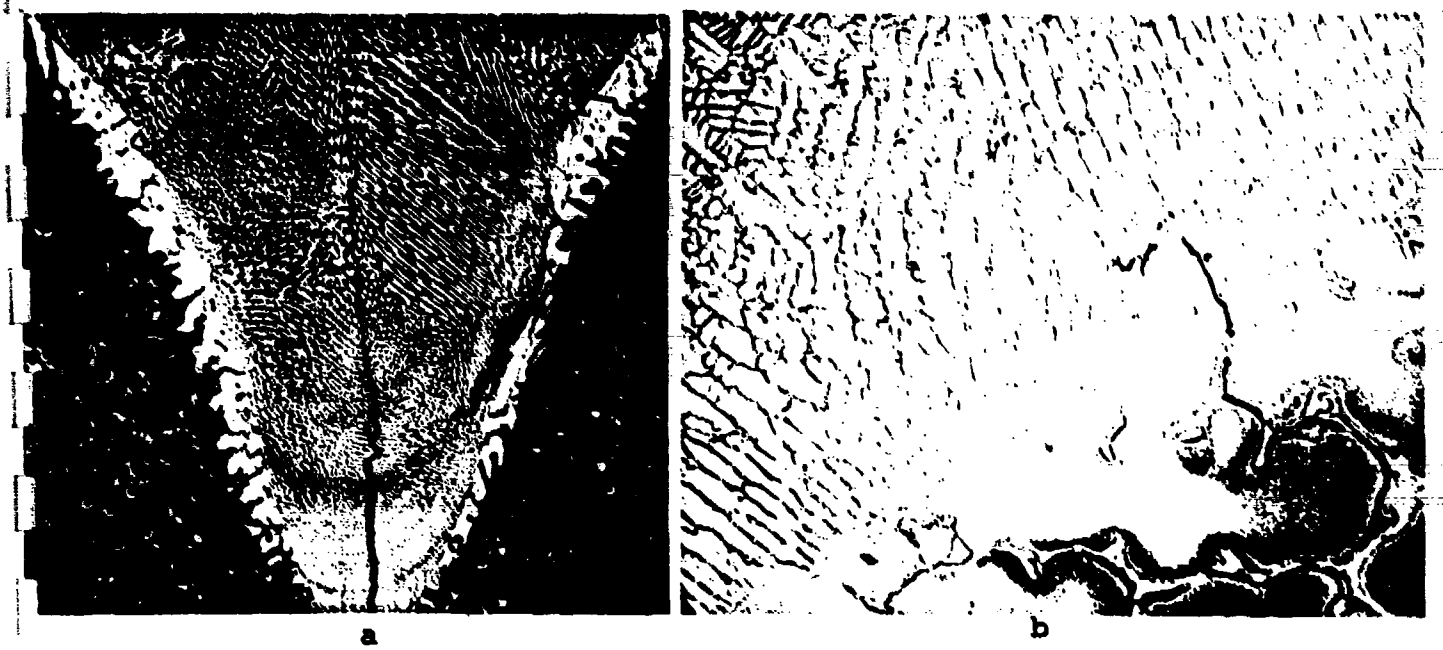

Fig. 29: Photomicrographs of transverse sections of an electron beam bead deposited at 0.8m/s. (a) 80X, (b) 400X. Ni-9.0wt%Al-4.0wt%Cr alloy.

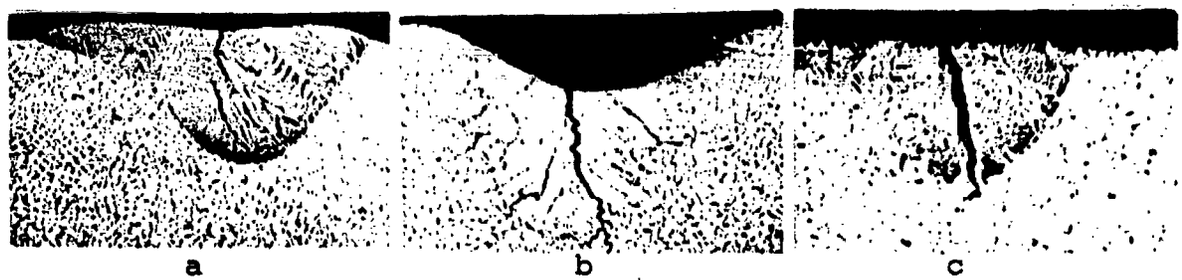

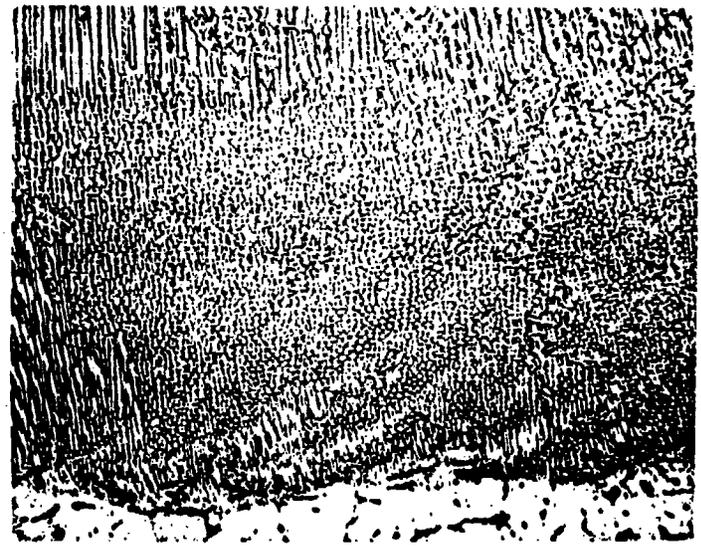

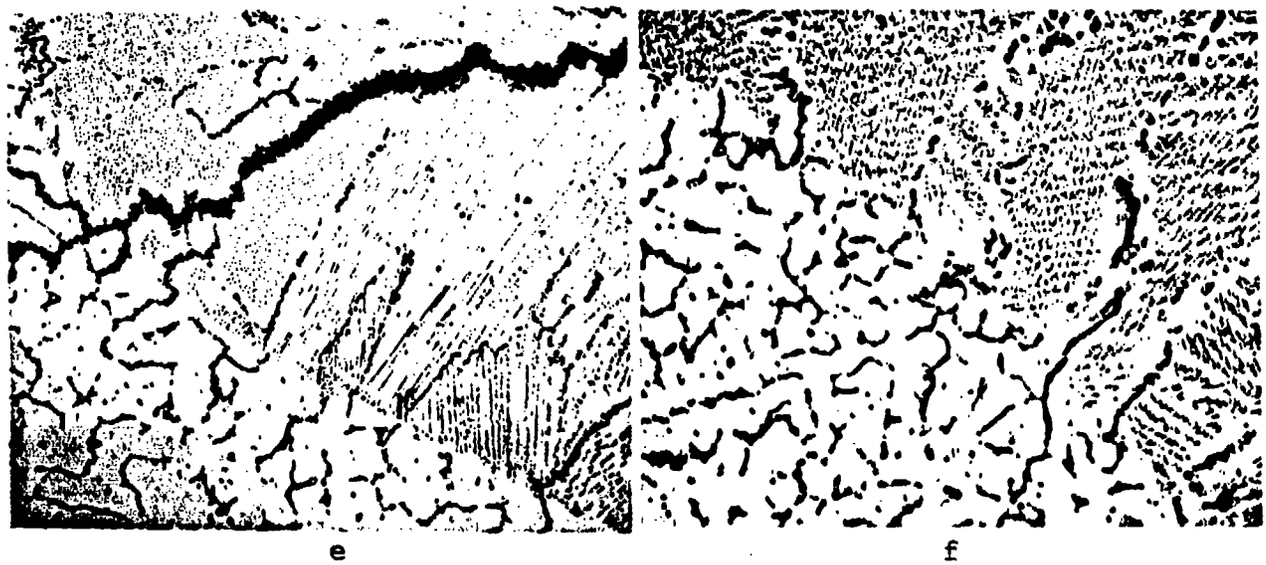

Fig. 30: Photomicrographs of transverse sections of electron beam beads deposited at 0.21m/s. As-solidified,(a) 80X,(d)400X. Homogenized at 1423K for 15 min. and air-cooled,(b)80X, (e) 400X. Homogenized at 1423K for 30 min. and air-cooled, (c) 80X and (f) 400X. Ni-9.0wt%Al-4.0wt%Cr-1.0wt%C alloy.

a

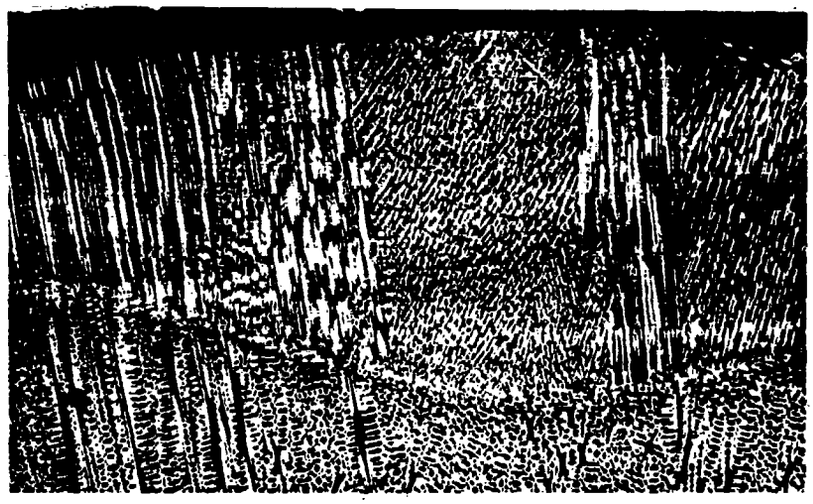

b

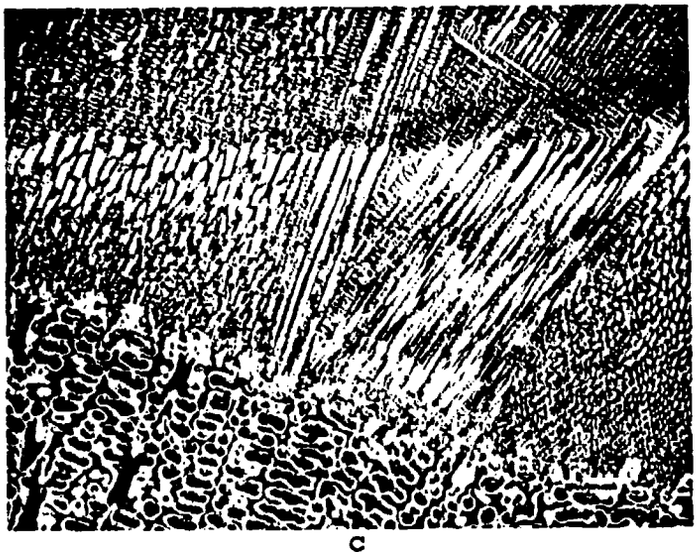

c

Fig. 31: Photomicrographs of longitudinal sections of an electron beam bead deposited at 0.21m/s. Ni-9.0wt%Al-4.0wt%Cr-1.0wt%B. (a) 80X, (b) 200X and (c) 400X.

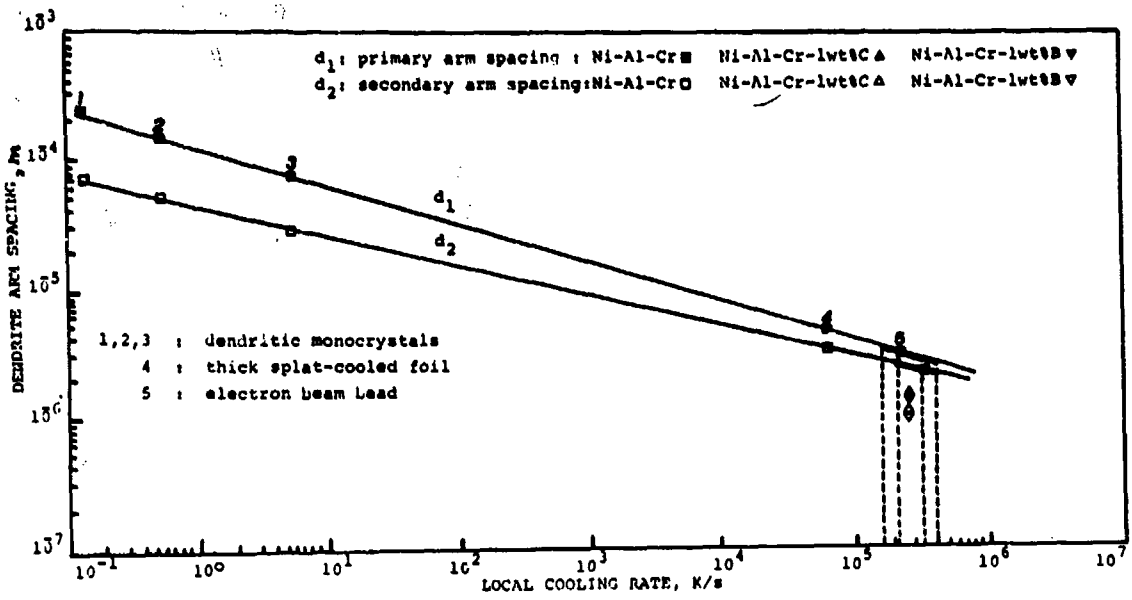

Fig. 32: Primary and secondary dendrite arm spacings versus local cooling rate. Ni-9.0wt%Al-4.0wt%Cr and the same alloy with 1.0wt%C or 1.0wt%B.

INSTITUTE OF MATERIALS SCIENCE

The Institute of Materials Science (IMS) was established at The University of Connecticut in 1966 in order to promote academic research programs in materials science. To provide requisite research laboratories and equipment, the State of Connecticut appropriated $5,000,000, which was augmented by over $2,000,000 in federal grants. To operate the Institute, the State Legislature appropriates over $500,000 annually for faculty and staff salaries, supplies and commodities, and supporting facilities such as an electronics shop, instrument shop, a reading room, etc. This core funding has enabled IMS to attract over $2,500,000 annually in direct grants from federal agencies and industrial sponsors.

IMS fosters interdisciplinary graduate programs in Alloy Science, Biomaterials, Corrosion Science, Crystal Science, Metallurgy, and Polymer Science. These programs are directed toward training graduate students while advancing the frontiers of knowledge and meeting current and long-range needs of our state and our nation.